Impedance Matching Networks for Wireless Applications

by

Raisa Georgiana Pesel

A thesis
presented to the University of Waterloo
in fulfillment of the
thesis requirement for the degree of
Master of Applied Science
in
Electrical and Computer Engineering

Waterloo, Ontario, Canada, 2014

© Raisa Georgiana Pesel 2014

I hereby declare that I am the sole author of this thesis. This is a true copy of the thesis, including any required final revisions, as accepted by my examiners.

I understand that my thesis may be made electronically available to the public.

Raisa Georgiana Pesel

Abstract

Impedance matching implies maximum power transfer from source to load as well as minimum signal reflection from the load, in an RF system. This explains the importance of impedance matching networks and their continuously increasing use in many electronic applications, as for example RF power amplifiers, source-pull and load-pull power transistor characterization or impedance matching devices such as Antenna Tuning Units.

The focus of this thesis is on the design, fabrication and test of impedance matching networks. Many different types of practical Impedance Matching Networks are available which is why detailed investigation and analysis are to be done in order to find the most suitable topology for the network. The analysis conducted in this sense indicates in favor of a Π-network topology consisting of a fixed inductor connected to two shunt variable capacitors, as tuning elements.

RF MicroElectroMechanical Systems (MEMS) switches are used to design a switch-capacitor bank for the proposed impedance matching network. Several RF switches are analyzed and simulated so that their behavior is known when applied to the capacitor bank. Multiple capacitor banks were designed and fabricated for the purpose of this thesis.

The MEMS-based approach provides better performance and wider capacitance ranges as compared to the conventional varactors. It allows the design of impedance matching circuits with different bandwidths and specifications, that can be used as part of a dynamically reconfigurable automatic match control circuit for a wide variety of wireless devices and intelligent RF front ends. For comparison purposes, an impedance matching network using commercial varactors is also simulated and its Smith Chart coverage is presented.

The designed circuits are fabricated and measured. The results indicate satisfactory performance and good agreement with circuit simulations.

Acknowledgements

Foremost, I would like to express my sincere gratitude to my supervisor, Professor Raafat Mansour, for accepting me in the Centre for Integrated RF Engineering (CIRFE) research group, for his continuous support, for his patience, motivation, enthusiasm, and immense knowledge. His guidance helped me in all the time of research and writing of this thesis. He is a tremendous mentor and it was a great honor for me to be his student.

Besides my advisor, I would also like to thank my committee members, Professor Mark Aagaard and Professor Hamed Majedi for reading my thesis and for all their insightful comments.

My sincere thanks go to Bill Jolley, Ahmed Abdel Aziz and Sara Attar for the time spent guiding me in the CIRFE lab and cleanroom, for their patience and kindness.

Many thanks to my dearest and magnificent friends Desireh Shojaei and Alexandra Sevastianova, for their priceless and unconditional support throughout all these years. Not to forget Mitra Gilasgar, who, although visiting UW for a short period, will be a life-long friend whose contribution to my wellness is unforgettable. I would also like to thank my officemate, Frank Jiang, and my good friend Oliver Wong for bearing with me and for all their constructive criticism and friendly advice. Also, all my other friends and colleagues are to be mentioned, many thanks for making my time in Waterloo enjoyable to Ehsan, Deanna, Baha, Humayra, Scott, Kevin, Mitra, Payam, Olzhas, Marco, Geff, Nazli, Saman and Grigory.

In particular, I am extremely grateful to Professor Mark Aagaard for trusting me, for his support and encouragement during my ECE 327 teaching assistantship experience, as well as during the writing of this thesis. His professionalism and ethics were a great inspiration and a model to follow in my future career.

Last but definitely not least, special thanks to my family. To my mother who played a key role in my decision to apply for the Master of Applied Science at University of Waterloo and who will always influence my career path. To my father who always ended up ceding to my demands. To my grandmother whose character strength I inherited. To my two sisters, my best friends, who were always there for me. And to my beautiful little niece who brought me light and joy and whose future I hope I can influence.

Dedication

This thesis is dedicated to my sisters for their support, encouragement and infinite love.

Table of Contents

List of Tables

List of Figures

Chapter 1

Introduction

1.1 Motivation

In order to minimize signal losses and provide good performance, a common goal of microwave devices is to maximize the power transmission from source to load and minimize the signal reflections. For this purpose, extensive research projects have been undertaken. The results prove the necessity of developing Impedance Matching Networks (IMNs) that can be used in RF power amplifier designs, as a stand-alone impedance tuner or as part of a dynamically reconfigurable automatic match control circuit for a wide variety of wireless applications and intelligent RF front ends.

In comparison with impedance transformers - that are terminated in a specific known impedance - impedance matching networks can generate a set of impedances by simply changing the state of some of the elements of the network.

It is well known that in wireless mobile communication systems, the input impedance of antennas is one of the most fluctuating parameters. It is a consequence of the environment variability and user interaction with the handset. [1] This is translated into detuned antennas with increased mismatch, decreased efficiency, and high power consumption of the system. Thus, IMNs are necessary in order to compensate for these changes and to allow tuning over a wide frequency band and to match the feed line impedance to that

of the transmitter, which is usually 50 Ω. The wide frequency band is important because with each variation, the antenna needs to appear as having a different electrical length and it must be tuned or made resonant at the required frequency. Otherwise, with no matching network, when the input impedance varies, there is a mismatch between the power module and the antenna, which brings in two major effects: first, the power module will not perform at optimal efficiency under load variations, and, second, the radiated power decreases due to the reflected power, so the equipment has to increase its power to compensate for the reduction. The result is an increase in the energy consumption (i.e., decreased battery endurance) or deterioration in the transmission quality. In addition, the power module could be damaged if the reflections of the signal levels are excessively high and no isolator is used. Also, it must be taken into account that, lately, all wireless systems tend towards increasing the number of frequency bands so that a higher data throughput and network capacity can be achieved. A well-designed impedance matching network could solve all these problems, extend battery endurance, achieve optimum output power, reduce weight for the same autonomy, or even increase the mobile range.

Today's wireless communication systems are using IMNs whose tuning elements are either solid-state varactors, switching p-i-n diodes or ferroelectric Barium Strontium Titanate (BST) varactors. Although BSTs offer a better RF linearity compared to the other options, at high frequency the quality factor of the matching network decreases and this attracts important disadvantages due to losses.

A new technology that is able to compensate for this drawback is related to the use of RF MicroElectroMechanical Systems (MEMS) switches when designing IMNs. This will improve the performance of the overall system due to the fact that RF MEMS are inherently low loss and are compatible with high frequency fabrication methods. Therefore the resulting matching networks can operate at relatively high frequencies and provide an improved impedance tuning range.

1.2 Objectives

The purpose of this thesis is to design, fabricate and simulate impedance matching networks and their tuning elements and prove the advantages of using the innovative RF MEMS approach in this process. In order to achieve this it is necessary to set and follow several objectives and divide the work into different stages, as presented below:

- **Analysis of impedance matching networks topologies:** Several different topologies are available and a deep understanding of each one of them is needed in order to choose the right one for specific applications. In this work, it is necessary to investigate and analyze the advantages and drawbacks of three proposed topologies and extract the most suitable approach.

- **Characterization of several RF MEMS switches that are to be integrated in the impedance matching network design:** As stated from the beginning, the interest of this thesis is focused towards the use of RF MEMS switches as part of the tuning elements for the impedance matching network. For this reason it is necessary to investigate their behavior in terms of the achievable capacitance range and quality factor, when connected in series with fixed capacitors.

- **Design and simulation of switch-capacitor banks and impedance matching networks using RF MEMS switches:** Since the final goal is the fabrication of such circuits, it is first necessary to simulate and optimize them in terms of reactive elements values, layout and overall dimensions. This is to be done through different software packages such as Advanced Design System (ADS)[1] and SONNET EM[2] simulator. Several sets of simulations are held for this purpose, starting from a rough design idea and ending with the final layouts that satisfy all requirements and that are to be further fabricated.

[1] ADS is a electronic design automation software for RF, microwave, and high speed digital applications. It allows both circuit and EM simulations and it provides fast and accurate first-pass design.

[2] SONNET is an accurate high frequency 3D EM simulator using the Method of Moments to provide accurate responses and results.

- **Fabrication and measurements of the switch-capacitor bank and impedance matching network:** RF MEMS are used to develop switch-capacitor banks that are to be further implemented in impedance matching networks used in wireless applications. These impedance matching networks must meet several requirements such as a wide tuning range, small size and low loss. The fabrication procedure of both the capacitor bank and the impedance matching network is part of the UW-MEMS process[3] held in the CIRFE lab at the University of Waterloo. Once fabricated, the proposed structures are to be measured and there must be good correlation between the simulation and measurement results so that the approach proves its sustainability.

1.3 Thesis Outline

Once the motivation and objectives are presented in Chapter 1, the thesis is further organized as follows. In Chapter 2 a study of different technologies and principles used in the design of several impedance matching networks is presented, along with the advantages that MEMS technology is introducing. Also, an overview on the applications of impedance matching networks has been carried out in this chapter. Next, Chapter 3 focuses on the characterization of the tuning elements that are to be used in the design approach chosen for the present work. Several types of RF MEMS switches are investigated and simulated in this sense. Chapter 4 is based on the design, simulation, fabrication and measurements of an impedance matching network and its tuning elements: a switch-capacitor bank that will play this role in the final structure. Different fabricated prototypes are proposed, each one of them showing specific characteristics. Based on this, their usage would depend on the desired application. Finally, a summary of the work done for the purpose of this thesis, along with the proposed future research plans are given in Chapter 5.

[3]UW-MEMS is a standardized multi-user surface micro-machined process, accessible to both industry and academia through CMC and completely administrated by CIRFE laboratory at University of Waterloo.

Chapter 2

Literature Survey

2.1 Impedance Matching Networks

Impedance matching networks are an extremely important component of many mobile wireless communication systems and devices where the signal can be easily affected by the external environment variations or by the user interaction with the handset. Also, as technology evolves, the tendency is to go towards higher frequencies and wider bandwidths, so there is a continuous need of changing the frequency band of operation, as well as the output power so that it keeps up with these requirements. The need of changing these parameters brings in the idea of tuning and impedance matching between different blocks of the communication systems so that a maximum power transfer, minimum reflections and higher efficiency of the system are achieved.

This topic has been continuously addressed over the years and extensive research was held concerning the design of impedance matching networks. The challenge in this context is in terms of deciding on what kind of tuning elements to use since several options became available with time and as expected, the performance in each case is different. Based on these different types of tuning elements, the impedance matching networks follow three types of tuning:

1. Electronic tuning using varactors and p-i-n diodes

2. Tuning using ferroelectric materials, BSTs

3. MEMS tuning

2.1.1 Electronic Tuning

In the early stages, varactors and p-i-n diodes were extensively used as tuning elements. For example in [2] a varactor-based matching network is considered, providing fast tuning and low distortion of the signal. Another example is illustrated in [3] where the authors propose a broadband impedance tuner having a microstrip load line and 10 stubs with varactors at each end, as illustrated in Figure 2.1. It can match a broad band of impedances, purely resistive as well as complex.

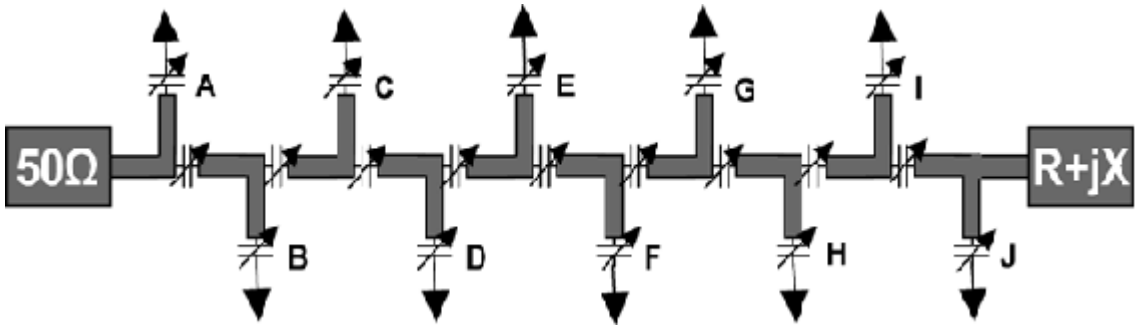

Figure 2.1: 10-stub impedance tuner [3]

Impedance matching networks for tunable filters are also discussed in [4] and [5] where varactor-based tuned bandpass filters are developed. In [4], a reconfigurable bandpass filter uses a combination of varactor diodes and ring resonators to provide good passband properties without requiring to shunt the tuning element to ground. The results obtained in this case prove the advantages that the coupling between resonating elements can bring when an increase in bandwidth is desirable. The combination of ring resonators and varactors makes the topic of [5] as well, where the authors describe the design process of a microstrip tunable bandpass filter. The ring resonator structure presents the advantage of not having any RF short circuited points as well as little radiation loss. Thus the performance of the filter is satisfactory, and a wide tuning range is achieved. A similar approach

is also discussed in [6] where the filter can be tuned from 2 GHz to 4 GHz with varactor diodes whose actuation voltage varies from 0V to 25V. The geometry of such a filter is shown in Figure 2.2 and it resembles the structures described in [4] and [5] as well.

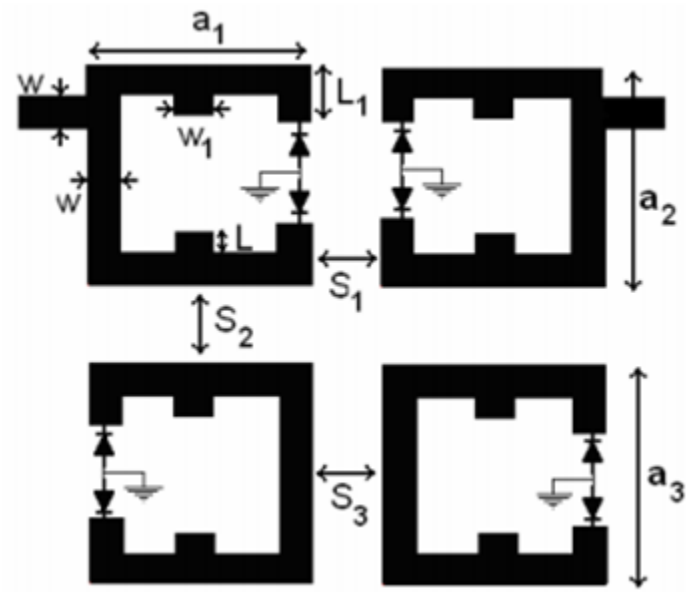

Figure 2.2: Ring resonator-based tunable bandpass filter [6]

A similar tuning mechanism is used in [7] where four varactors are used in order to introduce the variable capacitance and to modify the electrical length of the ring resonators. A structure using split ring resonators combined with comblines and loaded by varactors is proposed in [8]. The frequency range in this case is 800 - 1300 MHz and the results show that the combline structure introduces meaningful advantages in terms of bandwidth and tuning range, but it compromises the size of the structure.

A combination of three varactors and two microstrip quarter wavelength transformers is implemented in [9] where the results show that impedances ranging from 4 Ω to 392 Ω can be matched to a 50 Ω source at 2.25 GHz.

A reconfigurable impedance tuning network using lumped elements and electronically controlled tuning elements, positioned in a low-pass Π topology and meant for frequencies between 380 - 400 MHz, is described in [1]. This time, preference is given to p-i-n diodes

controlling fixed capacitors (Fig. 2.3), over varactors, due to the fact that varactors are not very suitable for high power applications. Hence, depending on the diode state, the fixed capacitors may or may not affect the capacitance of the overall circuit.
The network is simulated, fabricated and measured and the impedance dynamic range is shown in Figure 2.4 at 390 MHz.

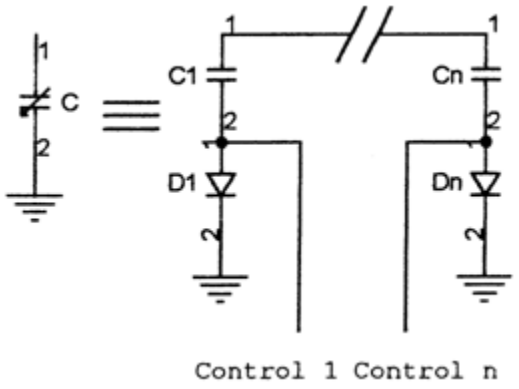

Figure 2.3: Replacement of the varactor [1]

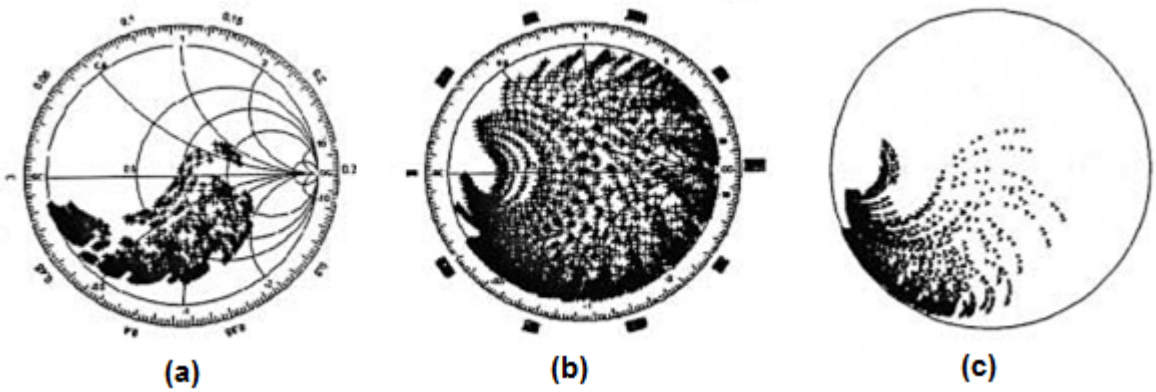

Figure 2.4: Impedance dynamic range: (a)Measurement results, (b) Simulation results with ideal components and (c) Simulation results with parasitic effects [1]

This paper represents one of the first instances where the complete picture of an intelligent RF control system was presented with the goal of impedance matching.

2.1.2 Tuning using ferroelectric materials

Regardless their fast tuning speeds, the reactive components used for electronic tuning present several drawbacks in terms of insertion loss, quality factor, linearity, and power handling. In order to overcome this, an alternative is to use thin-film ferroelectric varactors whose capacitance can be varied by changing the dielectric constant of the ferroelectric material. This is done by simply applying external bias voltage.

Thus, impedance matching networks, designed with BST varactors and providing low insertion loss, satisfactory quality factor, good linearity and good power handling capabilities were considered.

Using this approach, multiple research projects were developed over the years [10] - [19]. A tunable microstrip bandpass filter using BSTs is discussed in [10] where the authors report a combline structure (Fig. 2.5) developed on a sapphire substrate that is able to achieve 16% tuning of the center frequency, from 2.44 GHz to 2.88 GHz, when the bias voltage is increased from 0 to 200 V.

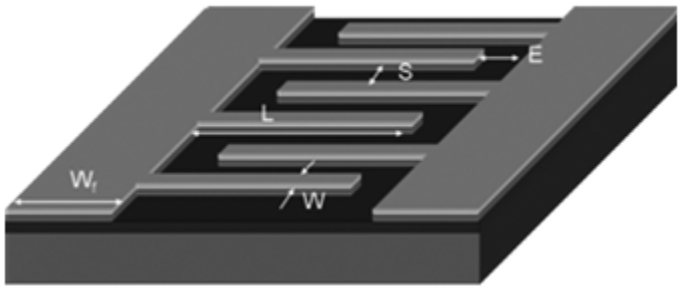

Figure 2.5: Interdigital BST varactor [10]

Tunable low-pass and bandpass filters are also discussed in [16] where 40% and 45% tunability is reached, respectively. For the low-pass configuration, a quality factor of 50 is achieved at 160 MHz, while the bandpass is giving a quality factor of 26 at 150 MHz. This is still higher than the quality factor provided by electronic tuning using varactors, with the same capacitance ranges as the BSTs discussed in this paper. The low loss tunable properties of BSTs were equally proven in [14] when applied to wireless and satellite

communication systems in low temperature environments.

This topic is discussed in [11] as well where a Π impedance matching network using BST varactors as tuning elements is designed. Its achieved impedance coverage is as shown in Figure 2.6.

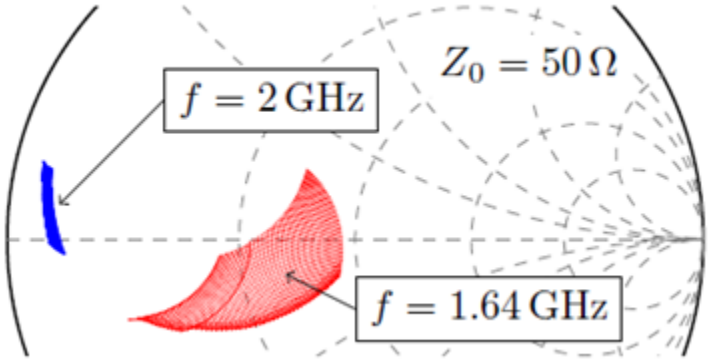

Figure 2.6: Impedance dynamic range of the matching network [11]

Tunable and flexible (Fig. 2.7) BST varactors are presented in [19] as inter-digital capacitors printed on a flexible substrate. They demonstrate good tunability, in the order of 22 - 28%, with quality factors as high as 80, for frequencies up to 50 GHz.

Figure 2.7: Flexible BST inter-digital capacitors [19]

Impedance matching networks using BSTs as tuning elements are implemented in the Blackberry Z10 [20] for tuning the antenna. This has a huge effect on improving the performance of the device, saving power, allowing a faster data upload and a decreased number of dropped calls.

(a)

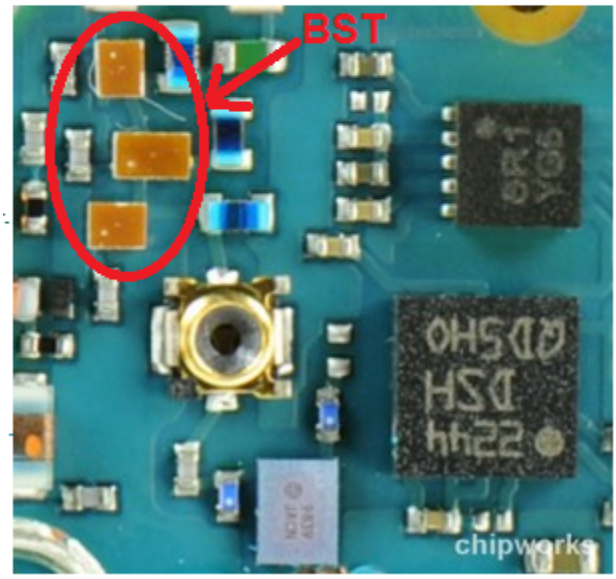

(b)

Figure 2.8: BlackBerry Z10: (a) Physical device and (b) Inside the device [20]

2.1.3 MEMS Tuning

As discussed in the previous sections, tuning was achieved using varactors, p-i-n diodes and BST capacitors. While the varactors and p-i-n diodes offer fast tuning speeds, they have significant drawbacks in terms of linearity, quality factor, and losses. All these can be improved by using BSTs whose fabrication techniques are very simple and cost effective. However, BSTs require high tuning voltages, which is not always easy or even convenient to provide.

In the past few years, RF MEMS switches, inherently low loss, have gained high appreciation, due to their ability of handling high power signal levels, providing excellent RF performance, and their compatibility with high frequency fabrication methods.

MEMS-based components such as tunable MEMS capacitors, MEMS capacitive switches, distributed MEMS transmission lines (DMTL) and switched-capacitor banks using MEMS switches are a few examples of structures that have been implemented in impedance matching networks, thus replacing the traditional varactors, p-i-n diodes or BSTs.

A series-LC matching network using RF MEMS capacitive switches is designed in [21]. The authors aim was for improved performance and link quality of cellular phones when used in variable environmental conditions. The structure of this network is presented in Figure 2.9 (a) and an example of matched load impedances at 900 MHz is shown in Figure 2.9 (b) where complex load impedances with values of 30; 50; 70 + j(-25; 0; +25;+50; +75) Ω are matched to approximately 30; 50; 70 Ω over the circle segments of constant resistance.

Examples of impedance matching networks involving RF MEMS switches are found in many recent research projects such as [22] - [28].

A reconfigurable power amplifier, including an adaptive matching network comprised of shunt MEMS switches in order to achieve variable capacitances, is presented in [24]. The frequencies of interest in this case are 6 GHz and 8 GHz. It is shown in this paper that the efficiency of power amplifiers can be improved if reconfigurable matching networks are used both at the input and output of the amplifier.

Reconfigurable double-stub tuners using MEMS switches are discussed in [22] where

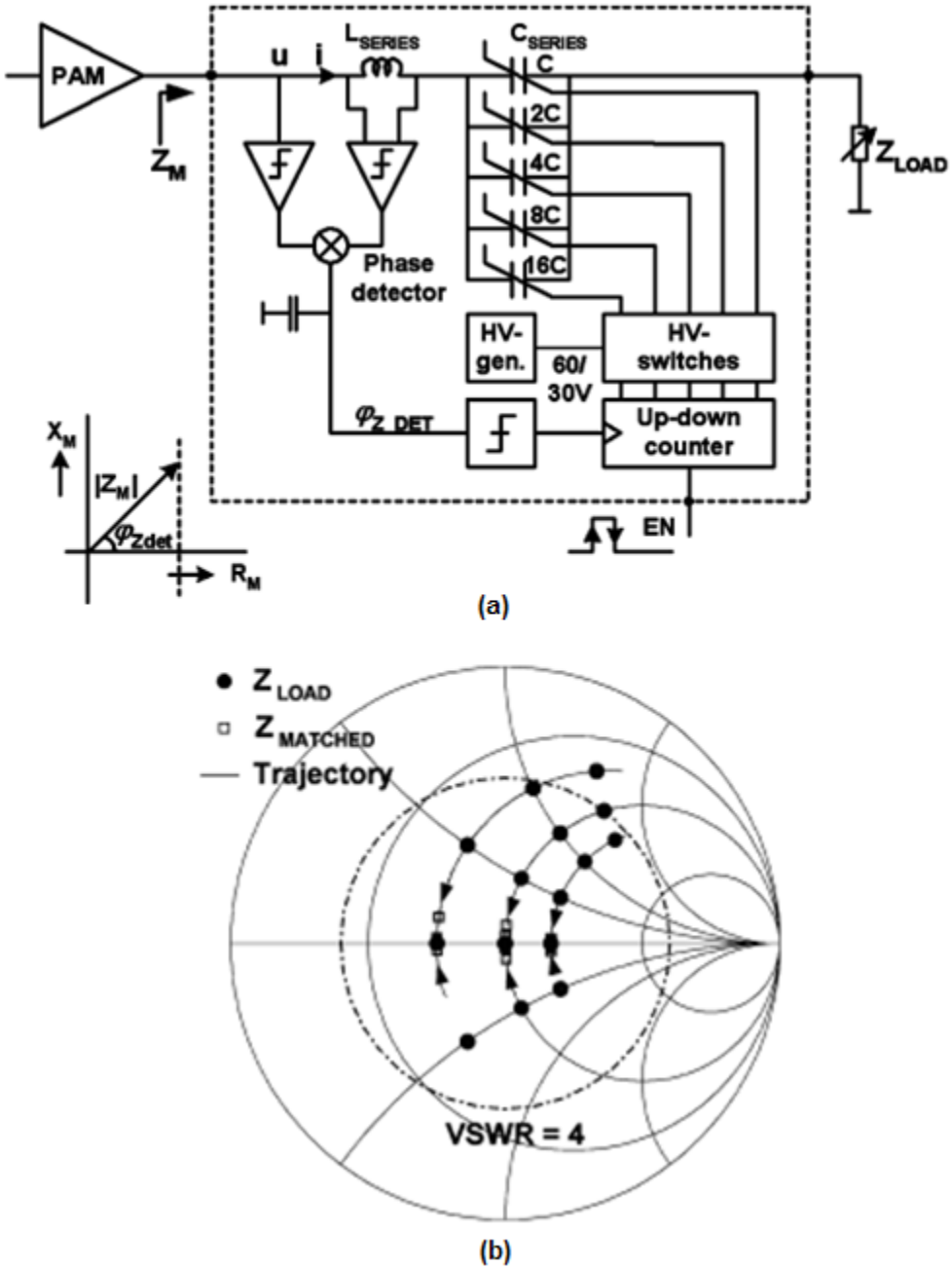

Figure 2.9: Impedance matching network: (a) Block diagram and (b) Impedance mismatch adaptation [21]

the structure can provide good matching over 10% - 15% of the bandwidth of a wide range of load impedances over a wide range of frequencies, in the order of 10 - 20 GHz. The impedance matching is accomplished with the aid of an RF MEMS switched-capacitor bank, illustrated in Figure 2.10, that is loading the stubs with different capacitance values, based on the state of the switches. This allows the selection of a discrete set of loads to be matched. Figure 2.11 shows the range of the matched load impedances. For this approach, there is a direct dependency between the values and number of capacitors and the range of load impedances that must be matched. In other words, a wider load impedance range may require additional capacitors and switches. The proposed approach shows good matching of complex load impedances, Z_L, ranging as shown in Table 2.1.

Table 2.1: Range of Load Impedances Being Matched

		$\mathbf{Re}(Z_L)$ [Ω]		$\mathbf{Im}(Z_L)$ [Ω]	
		min	max	min	max
f [GHz]	10	3	94	-260	91
	20	1.5	109	-107	48

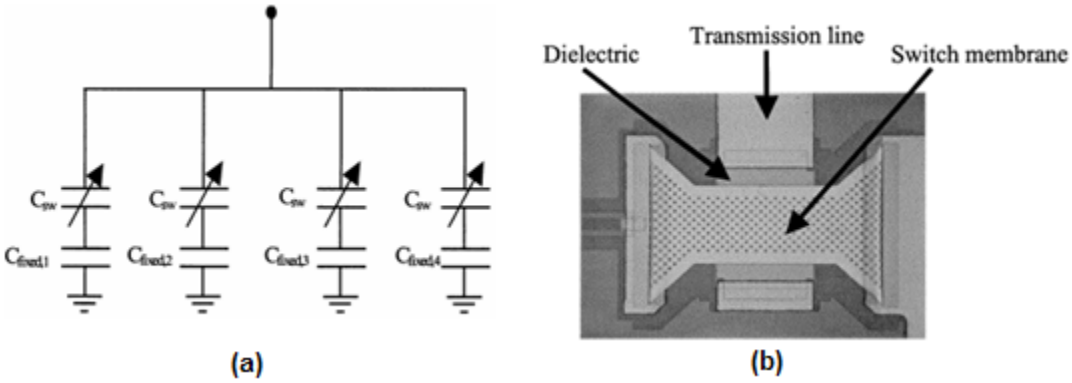

Figure 2.10: Switch capacitor bank: (a) Schematic and (b) Photograph of the capacitive switch used in the design [22]

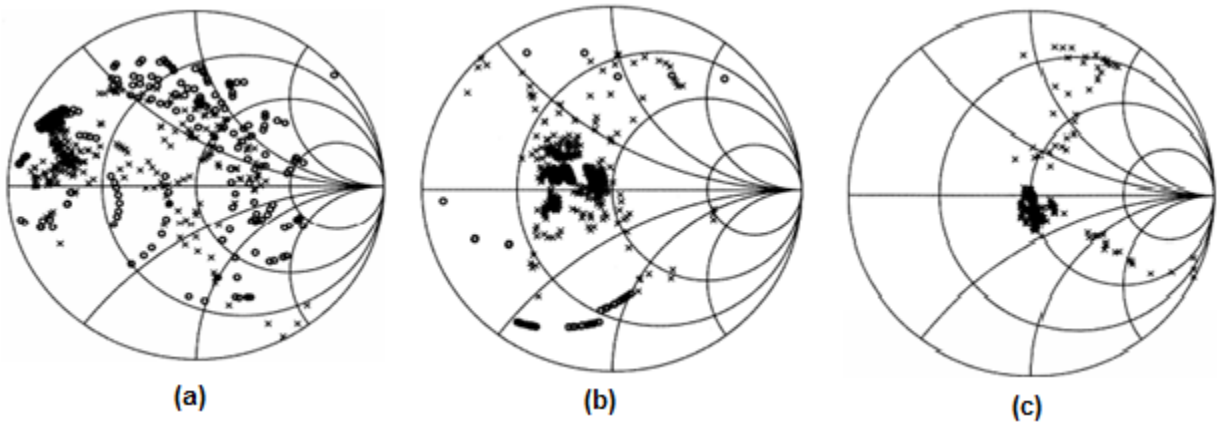

Figure 2.11: Simulated (o) and Measured (x) dynamic impedance range: (a) 20 GHz, (b)15 GHz and (c) 10 GHz [22]

A reconfigurable triple-stub impedance tuner using 11 MEMS switches as part of a capacitor bank, for frequencies ranging betwen 6 - 20 GHz is designed in [28]. The results show wide impedance matching as illustrated in Figure 2.12.

Extensive research in the field of impedance matching networks has been carried out in the CIRFE group as well [29] - [32].In [29] the authors propose a structure using MEMS series-contact switches and periodic defected-ground-structures (DGSs) implemented on coplanar waveguide (CPW) transmission lines. The DGS offer the advantages of an improved insertion loss and power handling capability, for frequencies up to 60 GHz, increasing the overall performance of the system so that a wide range of impedances is covered on the Smith Chart as it can be noticed in Figure 2.13.

RF MEMS switches demonstrate important advantages, such as low loss, high linearity, and the most important, low power consumption compared to the traditional varactors, diodes and BSTs. However, they are affected by self actuation at high RF power and by the increased temperature that the high power introduces.

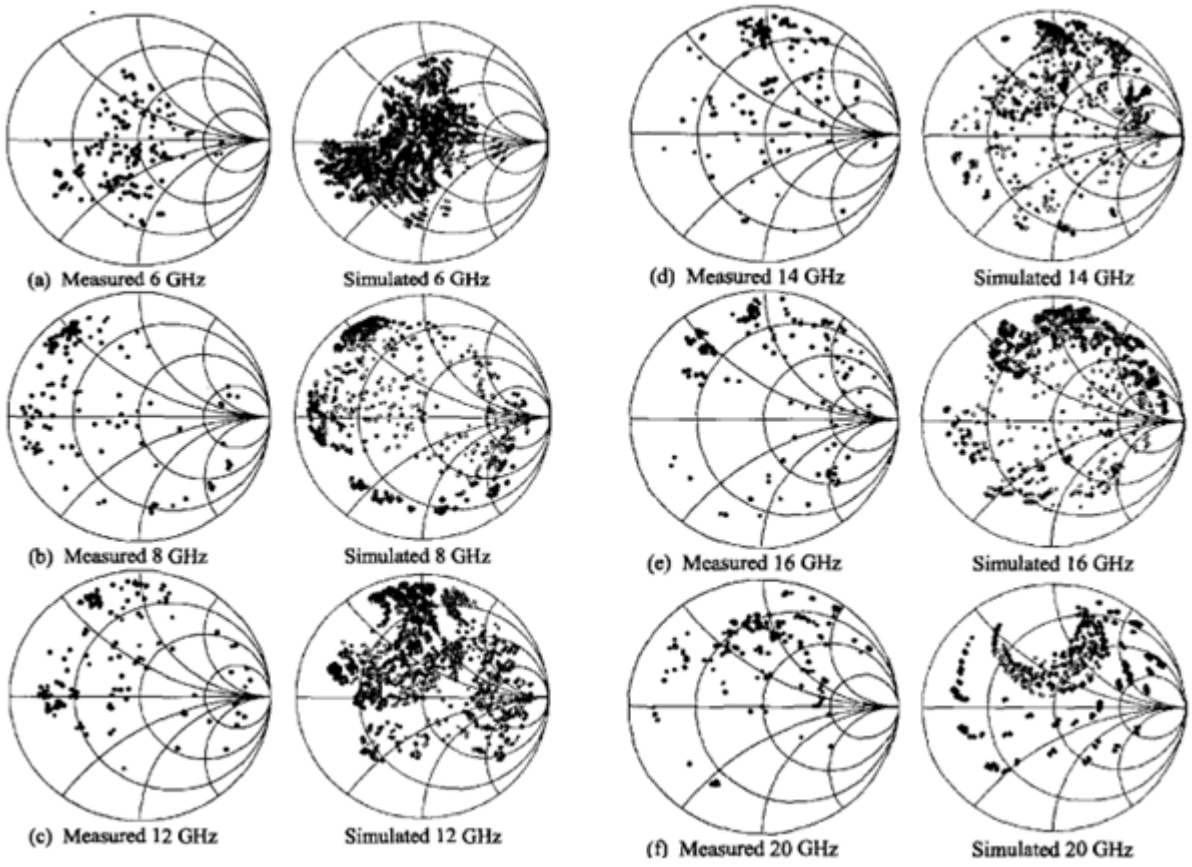

Figure 2.12: Dynamic impedance range of the designed matching network [28]

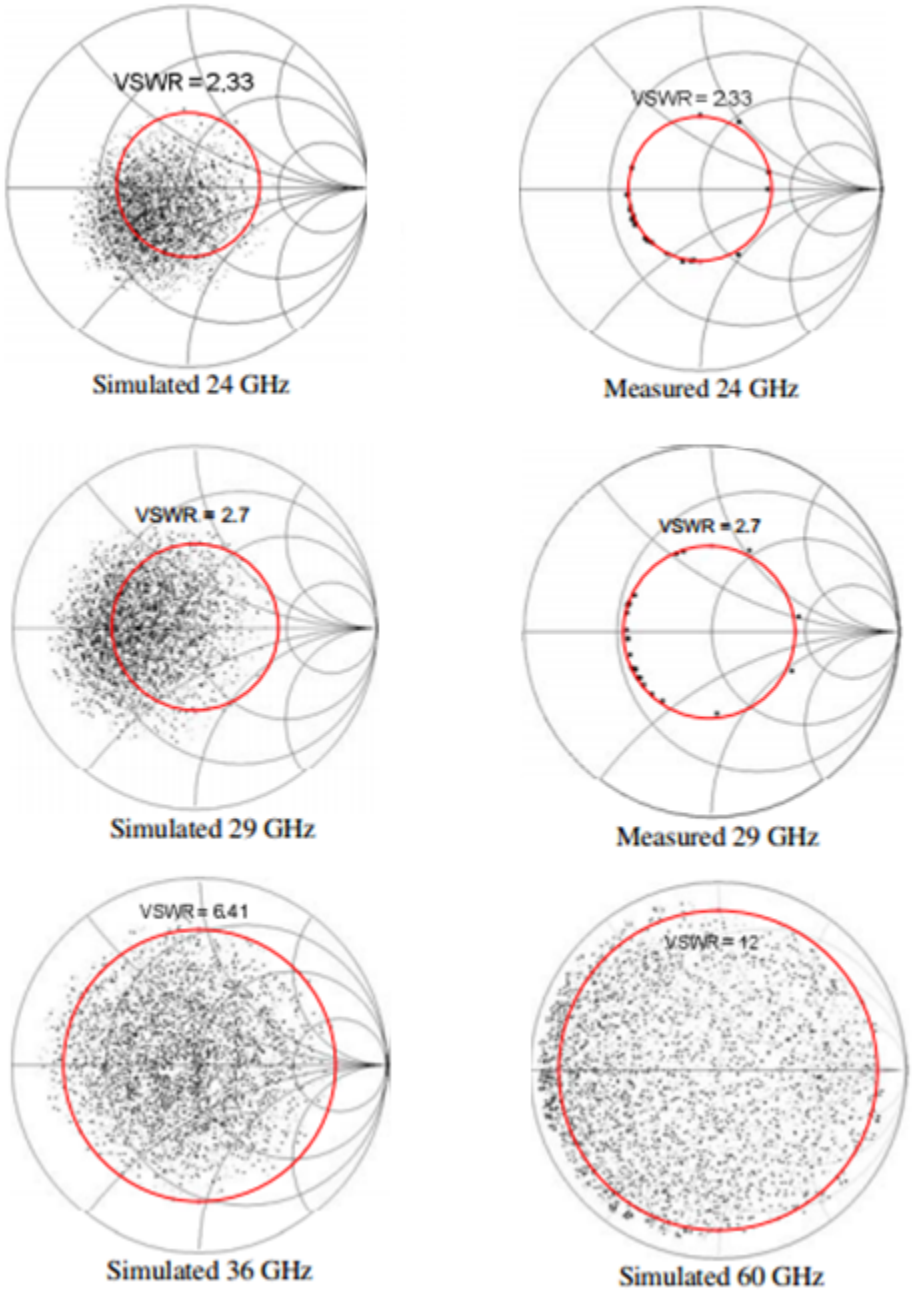

Figure 2.13: Dynamic impedance range of the designed matching network [29]

Chapter 3

RF Switches: Characterization of Tuning Elements

3.1 Introduction

Over the years, major research was held in the field of RF switches, due to their capability of routing the RF signal through one or more signal paths. Several advantages were demonstrated such as low losses, high quality factor, easiness of integration and suitability for applications in tunable filters, matching networks and antennas [33].

RF MEMS switches are particularly considered due to their ability of satisfying the linearity requirements of tunable networks in mobile applications. Switched capacitor banks are implemented using RF switches arrayed with fixed capacitors, this being an attractive alternative to the solid state devices used as tuning elements in many wireless applications, with frequency ranging from 800 MHz up to 5.8 GHz.

There are many examples of such capacitor banks in the literature, one of them would be as described in [34] where RF MEMS tunable capacitors, with low temperature sensitivity, are designed and fabricated on a quartz substrate. As a result, capacitance values ranging from 2.8 - 3.3 pF and a quality factor higher than 100 at 5 GHz are achieved. The same topic is discussed in [35] where a high Q tunable capacitor is designed and meant for 0.8 -

3 GHz applications. The device proves good functionality over the frequency range and it reaches capacitances varying between 1 - 3.8 pF for its different state configurations. Also, it maintains a quality factor higher than 60 at 2 GHz for all the tuning states. CMOS RF MEMS varactors were also discussed in [36] where the focus is on the switching time as well as on the achievement of higher self resonance frequencies with the proposed devices. In [37] the authors present an RF MEMS switched-capacitor suitable for both digital and analog tuning applications, for high frequencies, ranging between 1 - 10 GHz. A low-pass tunable filter is designed in [38], where the tuning elements are based on RF MEMS switches as part of a switched-capacitor bank. This capacitor bank is able to achieve capacitance values ranging from 0.96 - 8.69 pF for frequencies between 900 MHz - 5.8 GHz. Also, a high Q inductor is designed, whose inductance value is 2.22 nH at 5.8 GHz.

RF MEMS switches introduce improved performance in the systems due to their low insertion loss, excellent linearity performance, high isolation and low power consumption, thus becoming a better candidate than p-i-n diodes or BSTs for high frequency, wireless applications [39].

3.2 RF Switches based on SOI Technology

Although the present thesis is focusing on the RF MEMS switches, it is interesting to analyze the performance of SOI technology as well, for switches such as the ones proposed by Peregrine Semiconductor.

3.2.1 Peregrine switches

Peregrine Semiconductor[40] is the producer of high-end RF switches that offer very good performance in terms of linearity, power handling, high isolation, high electrostatic discharge (ESD) ratings, low insertion loss, low phase noise and small form factors. Most importantly, these switches are capable to operate over a wide frequency range. All these characteristics make Peregrine switches a great candidate for a broad range of applications

in aerospace and defense, in mobile wireless devices, test and measurement equipment or wireless-infrastructure markets.

One of their products is PE42556 [41], shown in Figure 3.1, an SPDT flip-chip RF switch, covering a wide frequency range, 9 kHz - 13.5 GHz, maintaining excellent RF performance and linearity over this range, and suitable for cellular and other wireless applications.

For a better understanding of the behavior of this switch at different temperatures, the manufacturer provides the performance plots shown in Figure 3.2. Using ADS, the same parameters are plotted at 25° C for comparison purposes only. The result is presented in Figure 3.3.

As mentioned in Chapter 1, one of the goals is to design a capacitor bank that is able to achieve a wide capacitance range and high quality factor using RF switches. In order to analyze these parameters, there are two equations that are used to plot the capacitance and quality factor:

$$C = 10^{12} * \frac{Im(Y_{11})}{2 * \pi * f} pF \tag{3.1}$$

$$Q = \left| \frac{Im(Y_{11})}{Re(Y_{11})} \right| \tag{3.2}$$

Where:

- Y refers to the input admittance parameters of the structure;
- f is the frequency.

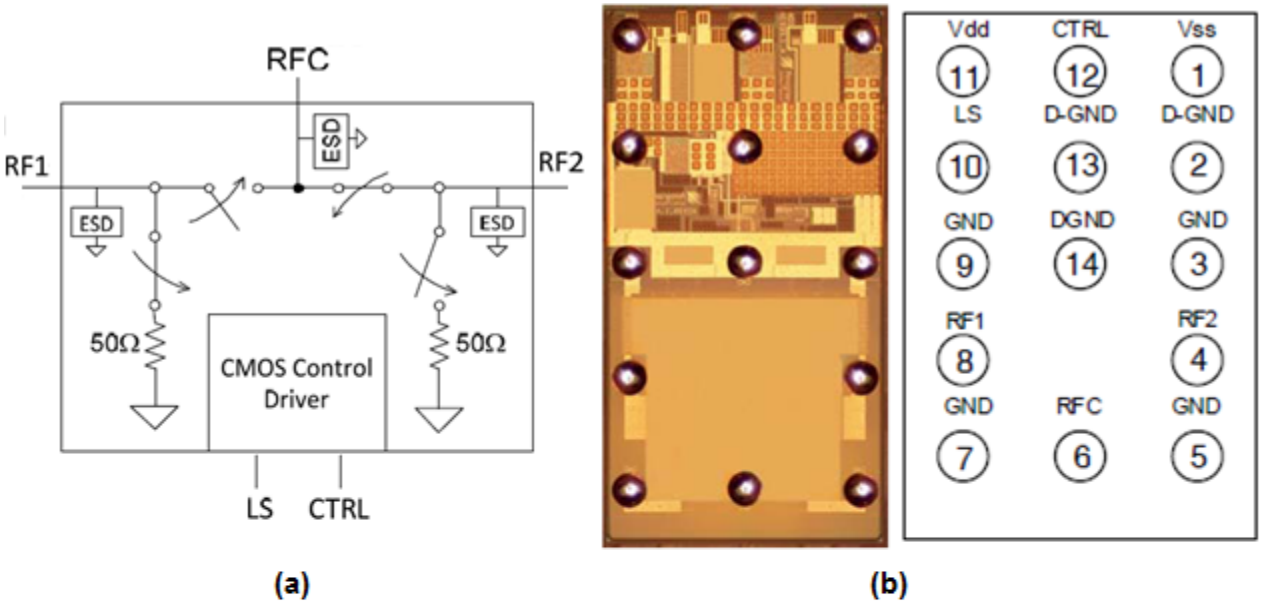

Bump No.	Bump Name	Description
1	V_{SS}	Negative supply voltage or GND connection (Note 3)
2, 13, 14	D-GND	Digital Ground
3, 5, 7, 9	GND	Ground
4	RF2	RF Port 2
6	RFC	RF Common
8	RF1	RF Port 1
10	LS	Logic Select - Used to determine the definition for the CTRL pin (see *Table 5*)
11	V_{DD}	Nominal 3.3V supply connection
12	CTRL	CMOS logic level

(c)

Figure 3.1: Peregrine SPDT RF switch: (a) Functional Diagram, (b) Flip-Chip Packaging and (c) Bump Description [41]

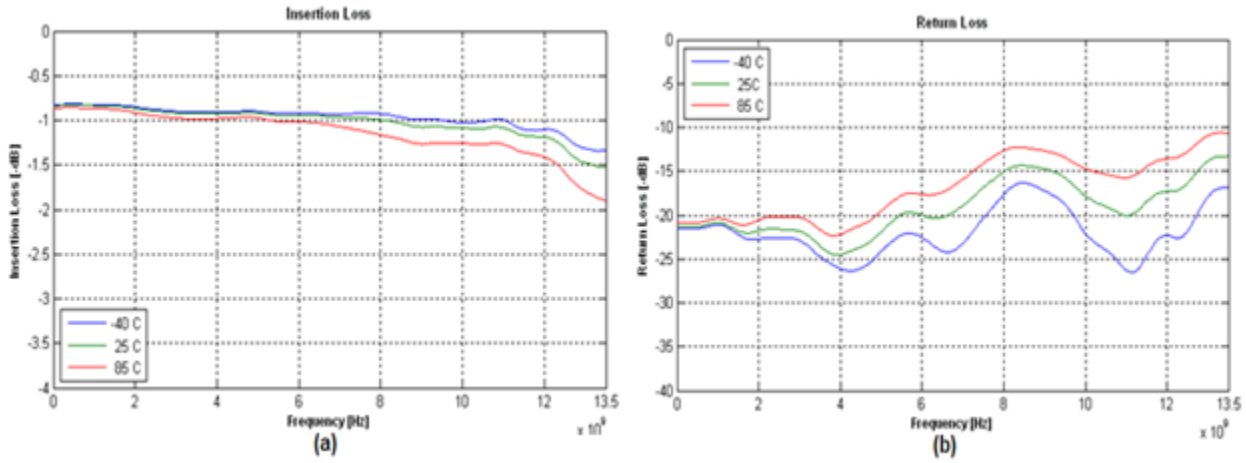

Figure 3.2: Peregrine SPDT RF switch - measurement results: (a) Insertion Loss and (b) Return Loss [41]

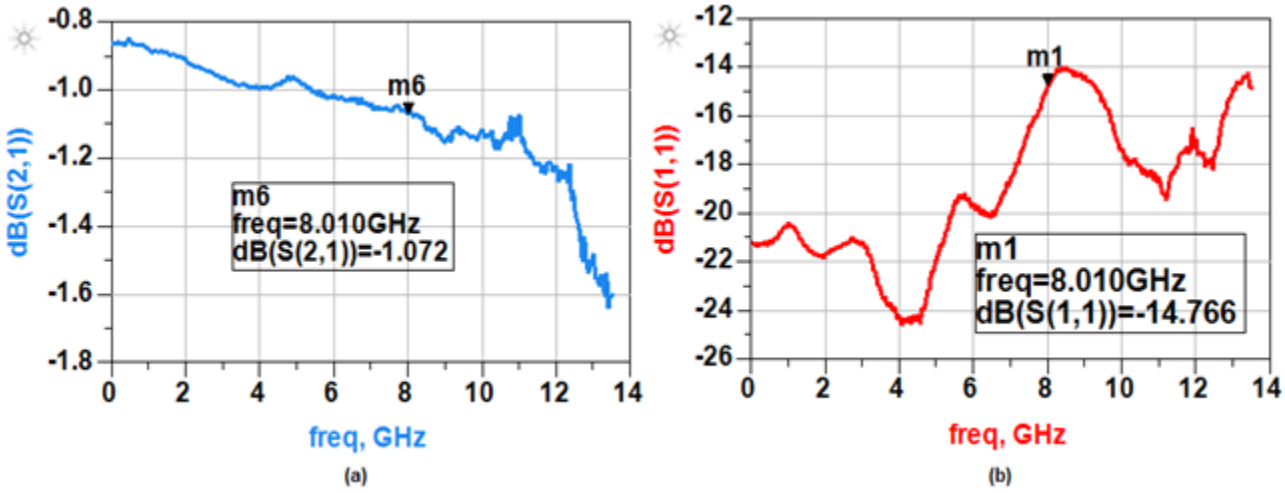

Figure 3.3: Peregrine SPDT RF switch - ADS simulation results at 25° C, generated using the supplied data file: (a) Insertion Loss and (b) Return Loss

For a deeper analysis and characterization, this switch is connected in series with fixed capacitors and further simulated in ADS, in terms of quality factor Q, and capacitance range C. The results shown in Fig. 3.4 correspond to the case when RF1 is in the ON state and RF2 is OFF so that C1=0.5pF receives RF signal, by being connected to the switch, and no RF signal passes through C2=1pF.

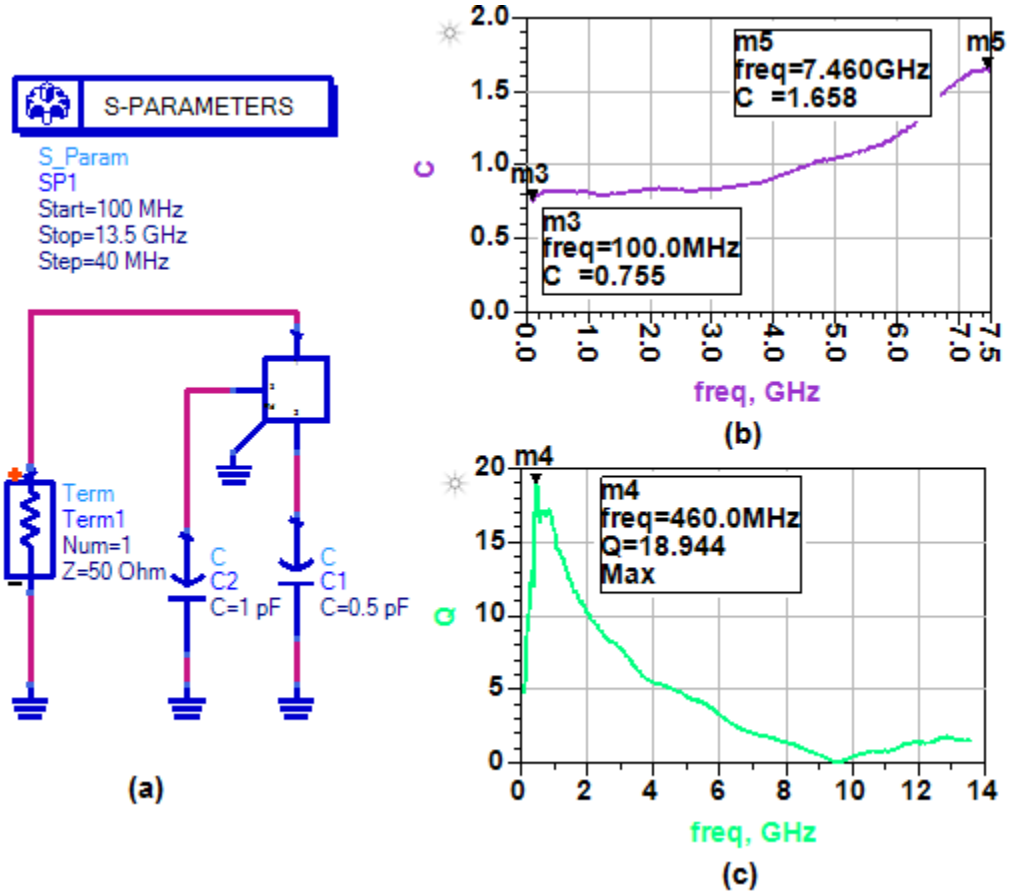

Figure 3.4: Peregrine SPDT RF switch: (a) Capacitor Bank, (b) Capacitance Range and (c) Quality Factor

It is easily noticeable that the input capacitance varies from 0.755 pF to 1.65 pF for frequencies below 8 GHz. The additional capacitance that is seen is attributed to the parasitic elements of the switch in the ON state.

Due to the packaging, the switch is much smaller than its direct competitors, it is directly positioned on the circuit board, and because of its short connection wires the inductance is greatly reduced, allowing higher-speed signals, and better heat conduction. However, the flip-chip packaging, renders this type of switch unsuitable for manual installation or replacement. Also, they require very flat surfaces on which to mount. This is not always easy to arrange or even maintain as the boards heat and cool repeatedly. Another drawback is introduced by the fact that the short connections are very stiff, so the thermal expansion of the chip must be matched to the supporting board or the connections could crack [42]. For these reasons it is decided not to go further with the analysis of this type of switch as it will not be used in the design of the switched-capacitor bank.

3.3 RF MEMS switches

There are many RF MEMS switches available in the industry, suitable for a variety of applications and able to meet diverse requirements. This section is focusing on two main commercial MEMS switches, produced by Omron and Radant, and it analyzes in detail the main characteristics of each one of them.

Since one of the declared objectives of this thesis is to design switch-capacitor banks using RF MEMS switches in series with fixed capacitors, it is interesting to see the capacitance range that can be achieved as well as the quality factor of such structures.

3.3.1 Omron switches

Omron Corporation[43] is a well-known manufacturer and provider of advanced electronic components, services and devices, whose area of expertise includes not only electronics, but industrial automation and healthcare as well. RF switches, connectors, MEMS flow sensors, pressure sensors, relays, as well as optical components are part of their developed products that are used in applications such as mobile communications, transportation, medical industry, appliance, consumer electronics, and test and measurement.

In the context of the present work, the focus of this section is on the 2SMES-01 Omron RF MEMS switch, a high frequency (up to 20 GHz), surface-mounted SPDT switch [44]. Its main features are low insertion/return loss and high isolation for GHz signals, small sizes (5.2 x 3.0 x 1.8 mm) and low power consumption (less than 10 μW). Figure 3.5 shows the performance of this switch in terms of insertion, isolation and return loss.

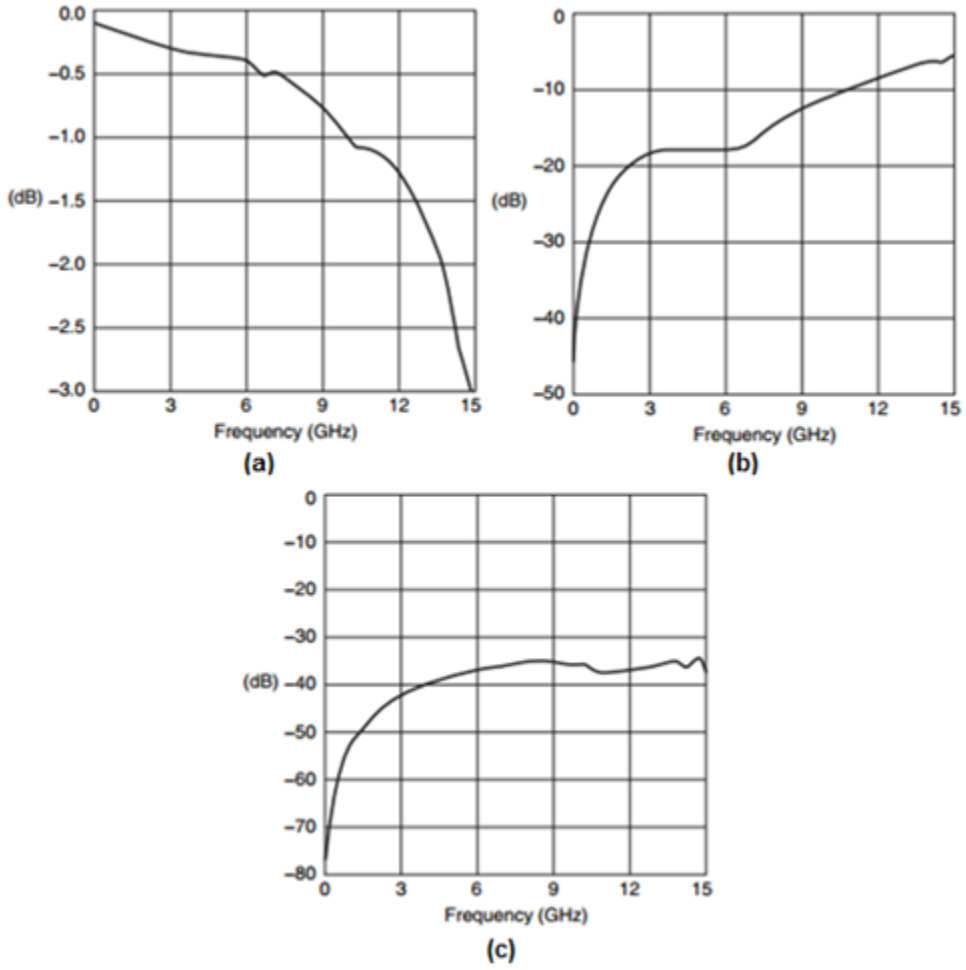

Figure 3.5: Omron SPDT switch - measurement results: (a) Insertion Loss, (b) Isolation and (c) Return Loss [44]

The same parameters are plotted in ADS from the supplied data file and the result is illustrated in Figure 3.6. If compared, it can be noticed that the measurement and simulation results are in good correlation.

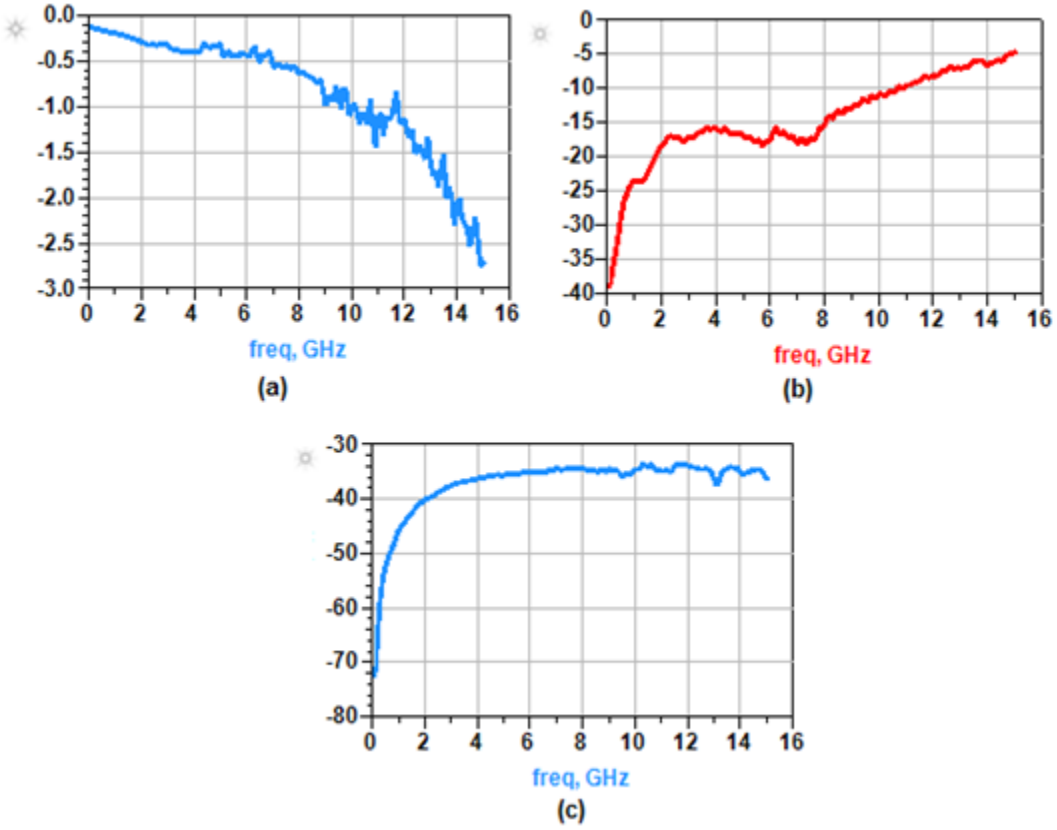

Figure 3.6: Omron SPDT switch - ADS simulation results generated using the supplied data file: (a) Insertion Loss, (b) Isolation and (c) Return Loss

Similar to the previous section, this switch is to be analyzed as well, in order to determine the capacitance range that it is able to achieve when connected in series with fixed capacitors. Thus, the capacitor bank shown in Figure 3.7 (a) is simulated. Due to the SPDT feature of the Omron switch, 16 capacitance states (Figure 3.7 (b)) can be achieved using only two of these switches.

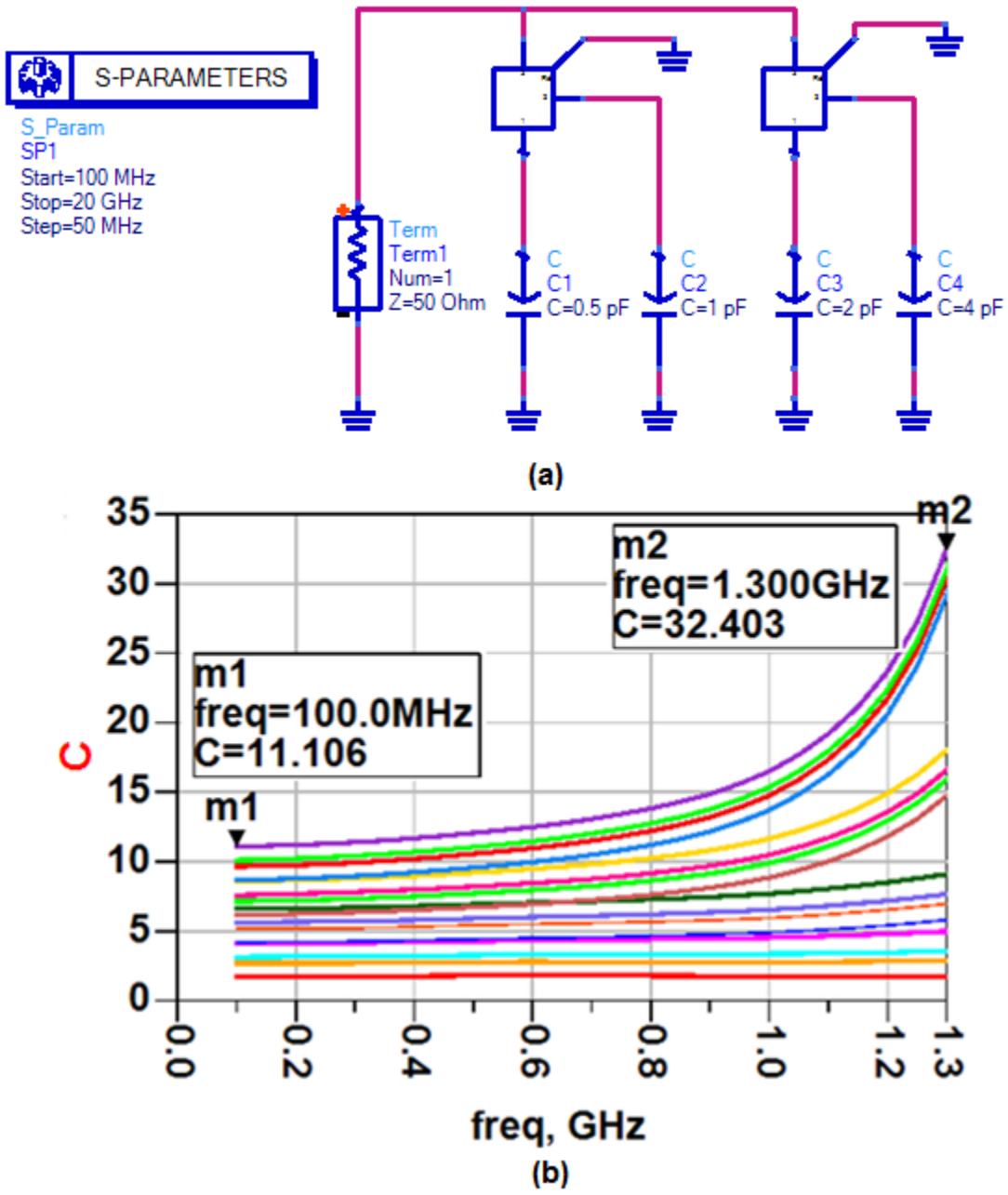

Figure 3.7: Omron SPDT RF MEMS switch: (a) Capacitor Bank and (b) Capacitance Range

As expected, very low capacitance values are achieved in the OFF state, around 1.6 - 1.7 pF, as opposed to the ON state, when all four fixed capacitors are connected, and high capacitance, ranging from 11 pF to 32 pF, is obtained.

3.3.2 Radant switches

Similar to Peregrine and Omron, Radant as well is an RF MEMS switches manufacturer [45], whose products meet the requirements for many governmental and commercial applications, including satellites, cell phones, and any microwave applications.

The main features of Radant RF MEMS switches include a validated lifetime of 100 billion cycles, low power consumption, high frequency functionality along with cost-effective packaging. They offer both SPST and SPDT versions of their switches so that based on the desired application and design requirements a choice is to be made in terms of the most convenient version.

Particular interest is given to one of their products, RMSW220HP [46], an SPDT high-frequency (up to 40GHz) switch providing high isolation, low insertion loss, and high linearity. Its packaging dimensions are 1.45 x 1.4 x 0.65 mm. All these characteristics render it suitable for many RF and microwave applications, in telecommunications or wireless access.

The typical RF performance of this Radant switch, given by the manufacturer, is presented in Figure 3.8. Using ADS, the same parameters are plotted, as shown in Figure 3.9. It can be noticed that the measurements match the ADS simulations.

Following the same procedure, this switch is used for the ADS design and simulation of the 16-state switched-capacitor bank shown in Figure 3.10 (a). Part (b) of the same figure illustrates the capacitance values obtained with the simulated capacitor bank.

As expected, the minimum capacitance values are achieved when both switches are OFF, and the maximum values, 9.1 - 38pF, are obtained for the case when both switches are in the ON state, so the RF signal reaches all four fixed capacitors.

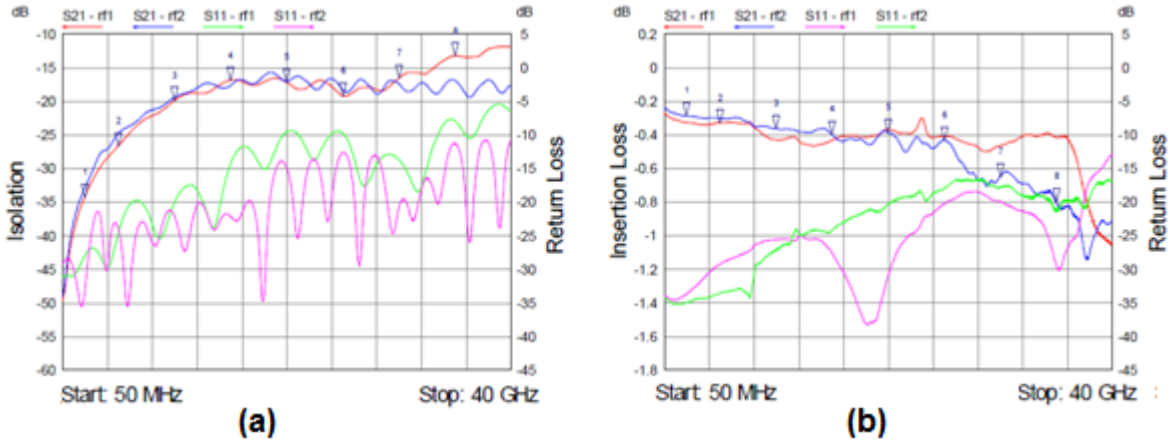

Figure 3.8: Radant SPDT switch - measurement results: (a) Isolation and (b) Insertion Loss [46]

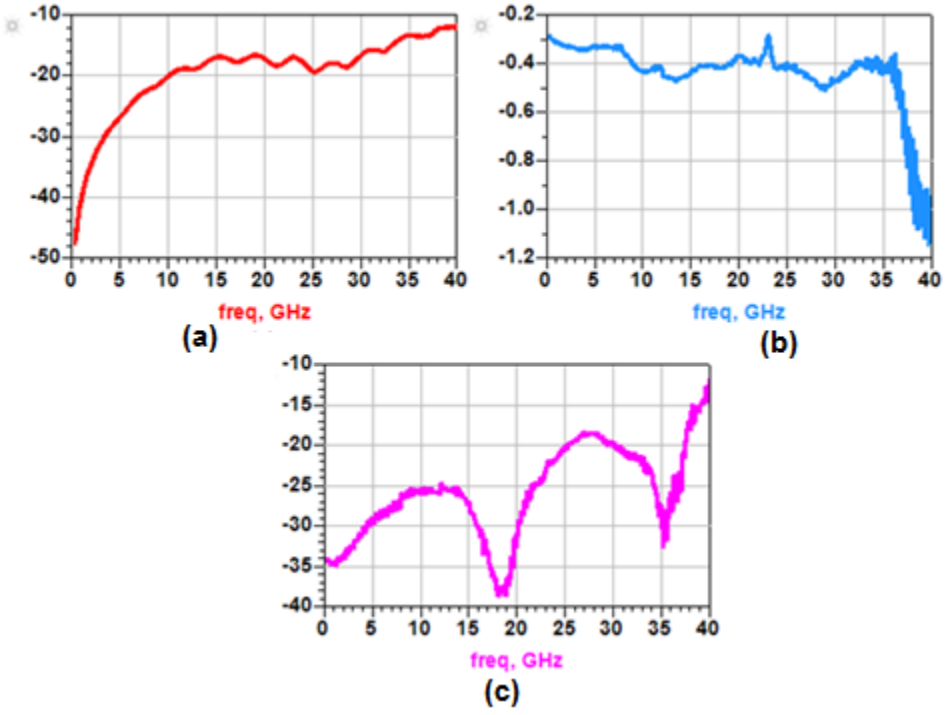

Figure 3.9: Radant SPDT switch - ADS simulation results generated using the supplied data file: (a) Isolation (b) Insertion and (c)Return Loss

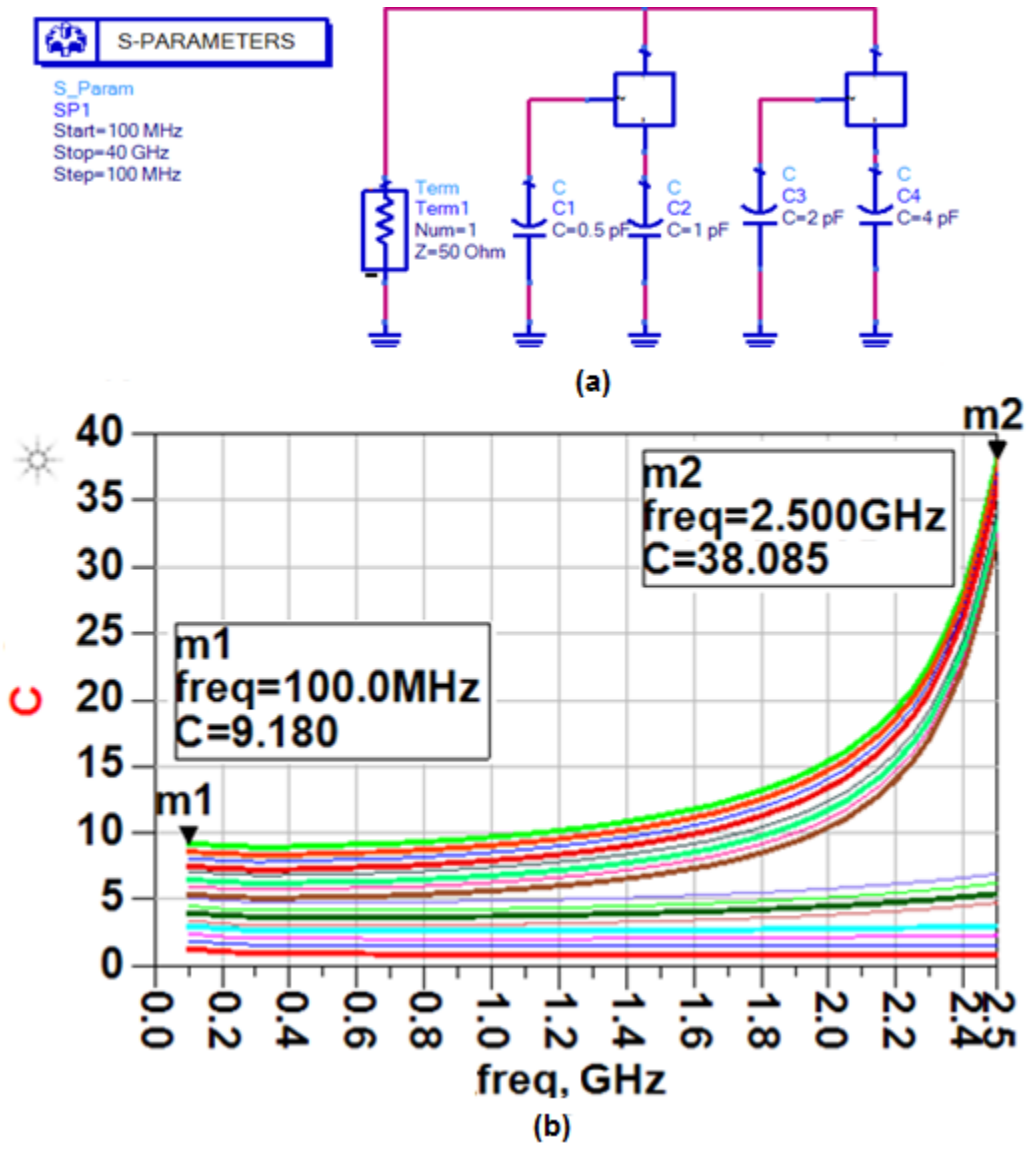

Figure 3.10: Radant SPDT RF MEMS switch: (a) Capacitor Bank and (b) Capacitance Range

3.4 Summary

The present chapter was concerned with the advantages that RF switches provide when used in wireless applications. The most important aspects are the low losses, high linearity, large tuning range, high frequency suitability, and low power consumption that such devices offer.

A short overview of several existing research projects on this topic was done. As a common point, all these projects proved the excellent reliability and properties of RF MEMS switches.

Further, the interest is focused on different types of switches: on one hand switches using SOI technology, and on the other, switches using the MEMS technology. In this context, RF switch from three suppliers, Peregrine, Omron and Radant are analyzed. Each one of them is proposing high-end products, with different packaging options, suitable for many types of applications and able to meet specific requirements. The intent is to analyze the capacitance range and quality factor that can be achieved by a 16-state switched-capacitor bank implemented using SPDT switches connected in series with fixed capacitors. The supplied data files are implemented in ADS in order to calculate the performance of these switched-capacitance banks over frequency.

One of the three discussed switches is to be chosen and further considered for the design and fabrication of the capacitor bank and for the design of the impedance matching network that will make the topic of the next chapter. Preference is given to the RF MEMS approach. However, in order to make this choice, multiple factors are taken into account, and the advantages and drawbacks of each one of these RF switches are weighed. Peregrine offers high performance but at the cost of complexity in implementation, due to its flip-chip packaging. Omron's packaging dimensions are as well challenging, and long wire bonds are needed for connections to the board. Radant with its small dimensions and pad placement seems to be the most suitable option for the purpose of the present work, and this is why it is the switch considered for the remaining of this thesis.

Chapter 4

Simulation and Fabrication of Impedance Matching Networks

4.1 Introduction

As discussed in the previous chapters, the use of IMNs has been of great importance over recent years due to the necessity of having mobile wireless devices functioning with wide bandwidths for different load conditions.

The general idea of impedance matching is shown in Figure 4.1 where a matching network is placed between the source and load. The matching network should ideally be lossless and able to transform the load impedance Z_L in the optimal working impedance of the signal source Z, and thus provide a maximum power transfer, minimum reflections from the load and automatically a minimum signal distortion [47]. For complex impedances, the maximum power transfer is achieved when Z equals the complex conjugate of the source impedance Z_S. Also, for an effective signal transmission it is necessary to maintain the amplitude and phase-frequency responses at some specific values, over a specific frequency range, in accordance with what is being transmitted. A well designed IMN could achieve these goals and provide satisfactory performance. For this purpose, it must be taken into account that, although ideally IMNs would match a set of source and load impedances, Z_0

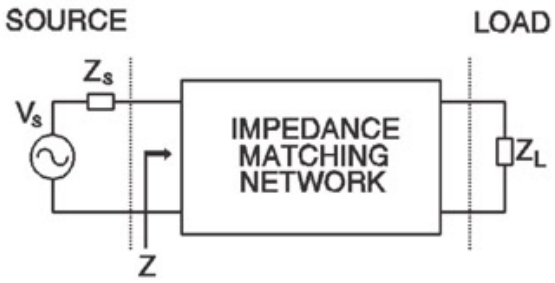

Figure 4.1: The general idea behind impedance matching

and Z_L, that are constant and do not vary with frequency, in most of the practical cases these impedances would actually vary with frequency and moreover, they would even vary at a fixed frequency. In order to start the design of an IMN, the first factor that needs to be considered is the choice of the topology of the network. As long as Z_L is not completely imaginary and it has some non-zero real part, there is always a corresponding matching network that can be found.

In this chapter, new types of impedance matching networks and their corresponding tuning elements are presented in terms of the design, simulation and fabrication processes. First, an overview on available topologies and principles of several impedance tuners is presented, as well as the design approach chosen for the present work. Once the most suitable topology is chosen, the next step is to investigate the feasibility of adding the tuning elements. In this sense, the approach of using RF MEMS switches to design switched-capacitor banks that would replace the conventional varactors is introduced. The complete layout design and measurement results of such capacitor banks are presented. The next section focuses on the design, simulation and measurements of the fabricated impedance matching network.

All the circuits discussed in this thesis are fabricated in the CIRFE Lab [48] at the University of Waterloo, using one of the main steps in the UW-MEMS process. An entire section is reserved to describe this fabrication process. The measurements are also carried out in the CIRFE lab and they agree with the simulations. The last section of this chapter stands for summarizing the conclusions.

4.2 Topology of the Impedance Matching Network

As previously stated, the choice of an appropriate topology for the matching network is an important factor in the overall design process. Several options are available and choosing one over another must be done after a thorough analysis of different factors such as [47]:

- Complexity: the simplest design satisfying the required specifications is preferred;
- Bandwidth: a perfect match can be obtained at a single frequency point with any type of matching networks. When a wider frequency band is desired a decision needs to be made regarding the type of matching network that is most suitable;
- Implementation and adjustability: depending on the intended application, the transmission lines and R/L/C elements, are to be considered.

There are three main types of matching network topologies: L, T and π, each one of them presenting uniques advantages as well as drawbacks.

4.2.1 L-network Topology

The simplest type is the L-network since it only uses two reactive tuning elements. They can be either inductors or capacitors arranged as the name states, in an L-shape. It has two possible configurations, as illustrated in Figure 4.2, based on the position of the normalized load impedance, z_L=Z_L/Z_0, relative to the 1+jx circle on the Smith Chart. Depending on the tuning elements, there are eight possible L - C combinations resulting in eight different L-matching networks. This approach is suitable for low frequency applications where commercial lumped-element capacitors and inductors offer good performance, but at higher frequencies the performance of the matching networks using such topology is affected. Also, although simple and very easy to implement, this topology exhibits the so-called "forbidden regions", as large areas on the Smith Chart, where the load impedances cannot be matched to 50 Ω. As an example, Figure 4.3 shows the yellow areas corresponding to the forbidden regions. So the use of this topology would be justified for very precise applications and well-known load impedances, to assure the good functionality away from these large forbidden regions.

Figure 4.2: L-topology impedance matching networks. (a) z_L inside the 1+jx circle and (b) z_L outside the 1+jx circle

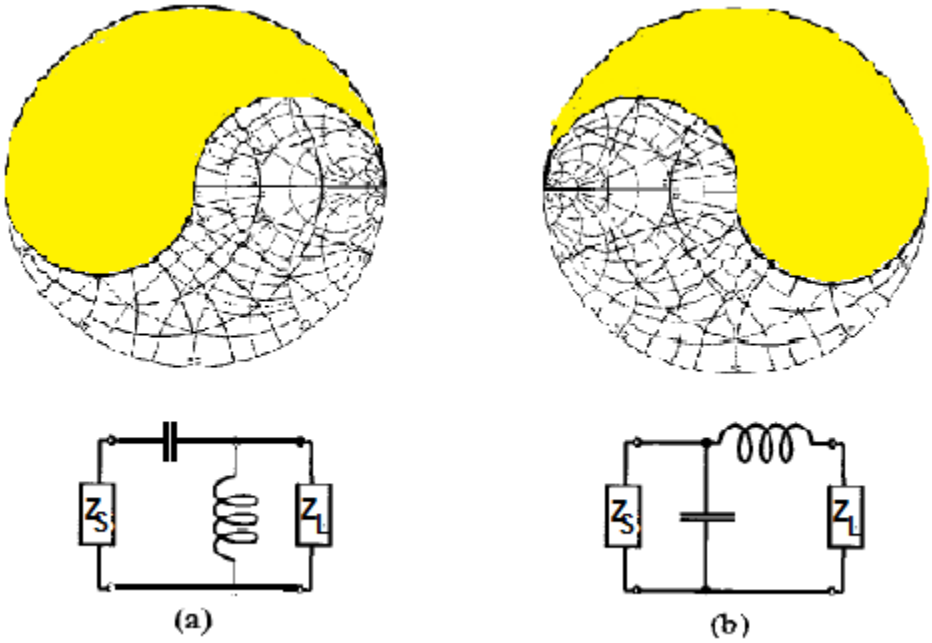

Figure 4.3: Forbidden regions for L-network topology with Z_S=Z_0=50 Ω . (a) z_L inside the 1+jx circle and (b) z_L outside the 1+jx circle

4.2.2 T-network Topology

In order to introduce an extra degree of freedom in the circuit, and better control of the quality factor, a third reactive element is added to the previously discussed L-network and arranged in a configuration similar to the letter T, thus obtaining the T-network topology, as illustrated in Figure 4.4.

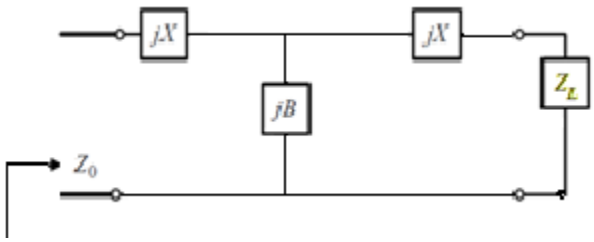

Figure 4.4: T-topology impedance matching network

This type of network is extensively used in mobile communications systems due to its ability to offer a wide impedance coverage, along with good linearity and small circuit sizes. The T configuration also presents the advantage that the two series elements have one node inherently grounded and the tuning voltages can be applied independently via external networks as shown in [49]. Also, based on the application requirements, as proven in [50], T-matching networks are most suitable for matching high impedances.

4.2.3 Π-network Topology

Similar to T-networks, the Π-topology is also a three-L-C-element circuit as shown in Figure 4.5. Over the years, preference was given to these networks due to their ability to offer better flexibility when a wide range of frequencies is required and the fact that they can provide good response to the rapidly changing impedances.The above-mentioned flexibility offers many tuning possibilities and allows the synthesis of any complex impedance. The Π-network topology has been widely used in literature as the basic structure for impedance matching networks.

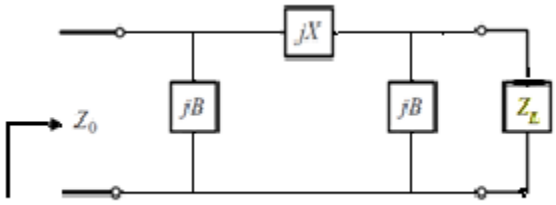

Figure 4.5: Π-topology impedance matching network

Based on the positioning of the reactive tuning elements, this structure can be translated into a low-pass network, when having an inductor in series with two shunt variable capacitors, or a high-pass, when using one capacitor in series with two shunt variable inductors. Figure 4.6 presents these two configurations.

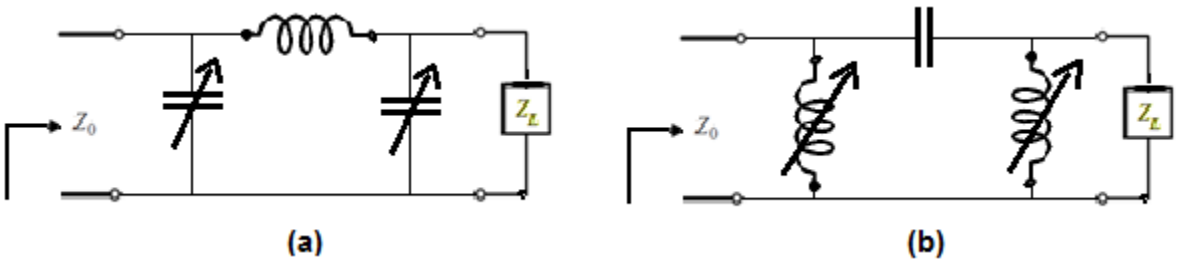

Figure 4.6: Π-network topology. (a) Low-pass network using variable capacitors and (b) High-pass network using variable inductors

The high-pass configuration shown in Figure 4.6 (b), using the variable inductors as tuning elements, is not a common practice, since these elements are in a very early stage of development. They are very expensive and present a significant drawback in terms of size.

On the other hand, the low-pass configuration, shown in Figure 4.6 (a), is the typical topology used in impedance matching networks for mobile wireless applications. Varactors and p-i-n diodes, in the early research projects [1], and further Barium-Strontium-Titanate (BST) varactors [51], were extensively used to achieve the desired variable capacitors. As a result, these components would ideally allow a very wide tuning range, but would need

analog control circuitry in order to control the final device. Most importantly, they are usually suitable for low RF power range. Since today's tendency is going towards high RF power, higher frequencies and wider bandwidths, the above mentioned components are not completely suitable anymore, due to their increased nonlinearity, higher losses, low quality factor and high noise figure.

In order to compensate for these drawbacks, the need of designing more advanced tuning elements appeared. RF MEMS switches are a good alternative for this purpose since they provide good performance in terms of linearity, loss and power handling.

The next section tackles this subject addressing the use of RF switched-capacitor banks in order to achieve desired capacity ranges.

4.3 Tuning elements: Switched Capacitor Bank

As stated above, RF MEMS switches, implemented in capacitor banks, have the capability of providing better performance in mobile wireless applications than their predecessors, the commercial varactors, p-i-n diodes or BSTs.

The present section is concerned with the design of such capacitor banks using the commercially available Radant switches illustrated in Figure 4.7 and characterized in Chapter 3. For obvious reasons, mainly related to the size of the final device, an SPDT Radant switch is preferred over an SPST version. Its datasheet provides all the necessary information in terms of pads and ground positioning, - Figure 4.7 (a) and (b)-, as well as showing the way of achieving the DC bias using a resistor RS or RD (40 KΩ - 100 KΩ) or inductor LS or LD respectively, as it can be seen in Figure 4.7 (c). Part (d) of the same figure is for assembly purposes only, to show how the DC bias would be realized for the switch that is to be further connected in series with fixed capacitors.

This being said, the goal is to obtain a 16-state switch-capacitor bank, using SPDT Radant switches. Each switch is to be connected in series with a fixed capacitor, as shown in Figure 4.8 (b). The values chosen for these capacitors are as follows: C1=C=0.5pF, C2=2C=1pF, C3=4C=2pF and C4=8C=4pF.

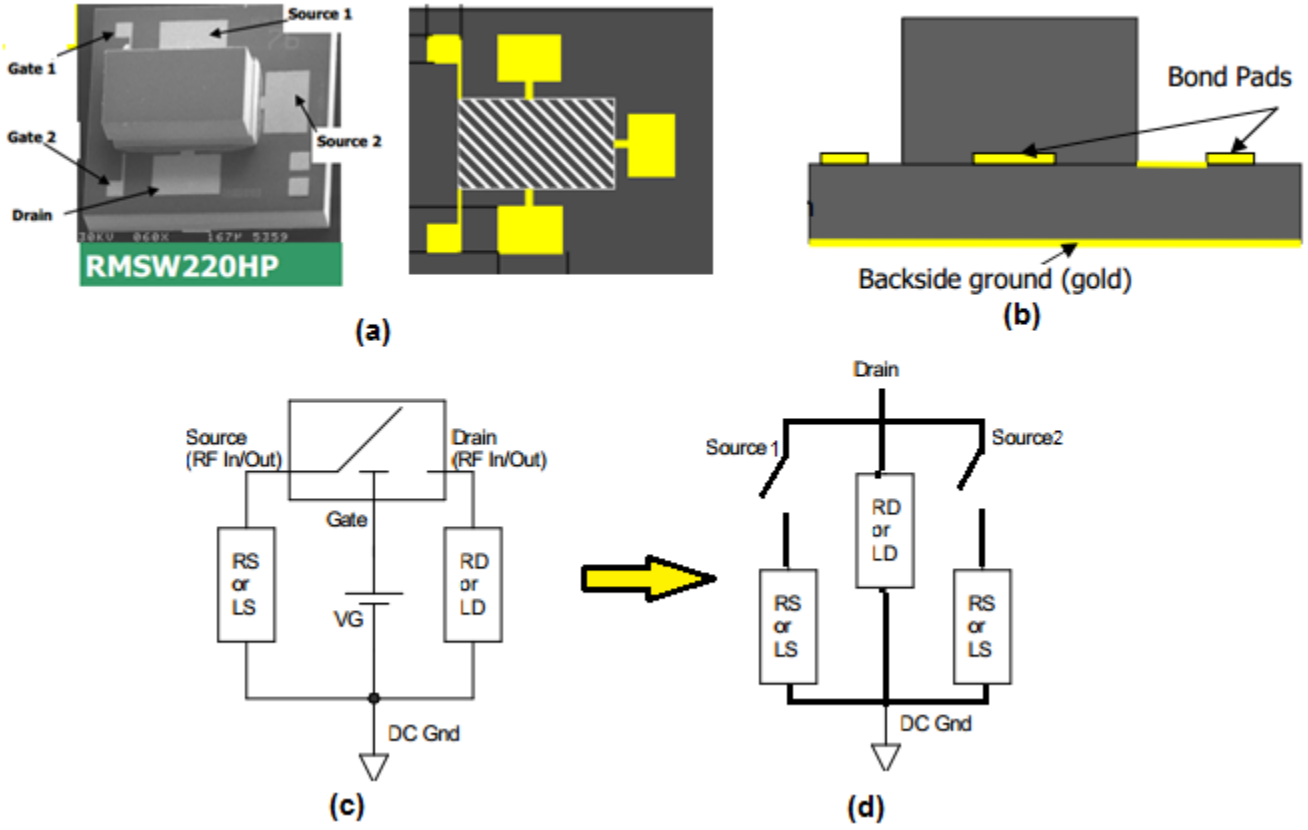

Figure 4.7: Radant SPDT switch: (a) top view (b) side view (c) half of SPDT switch as recommended application and (d) assembly recommendation [46]

Figure 4.8 (a) is for illustrative purposes only, to show that the capacitor bank can be implemented with use of SPST switches as well.

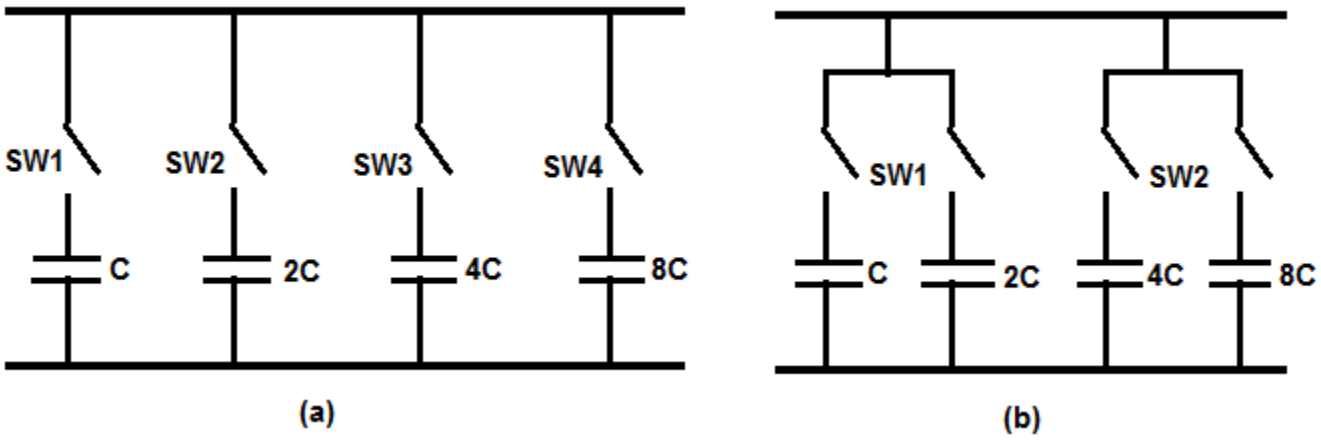

Figure 4.8: Basic idea of 16-state switch-capacitor bank: (a) using SPST switches and (b) using SPDT switches

4.3.1 Sonnet Layout Design and Simulation of the Capacitor Bank

For the design of this capacitor bank, as well as for the rest of the circuits fabricated for the purpose of this thesis, it is decided that 50 Ω Coplanar Waveguide (CPW) transmission lines be used since the UW-MEMS fabrication process does not allow the implementation of substrate via holes. The LineCalc tool from ADS is used to calculate the dimensions of the gap and signal line of the CPW, given the desired 50 Ω impedance, frequency and substrate characteristics, as illustrated in Figure 4.9.

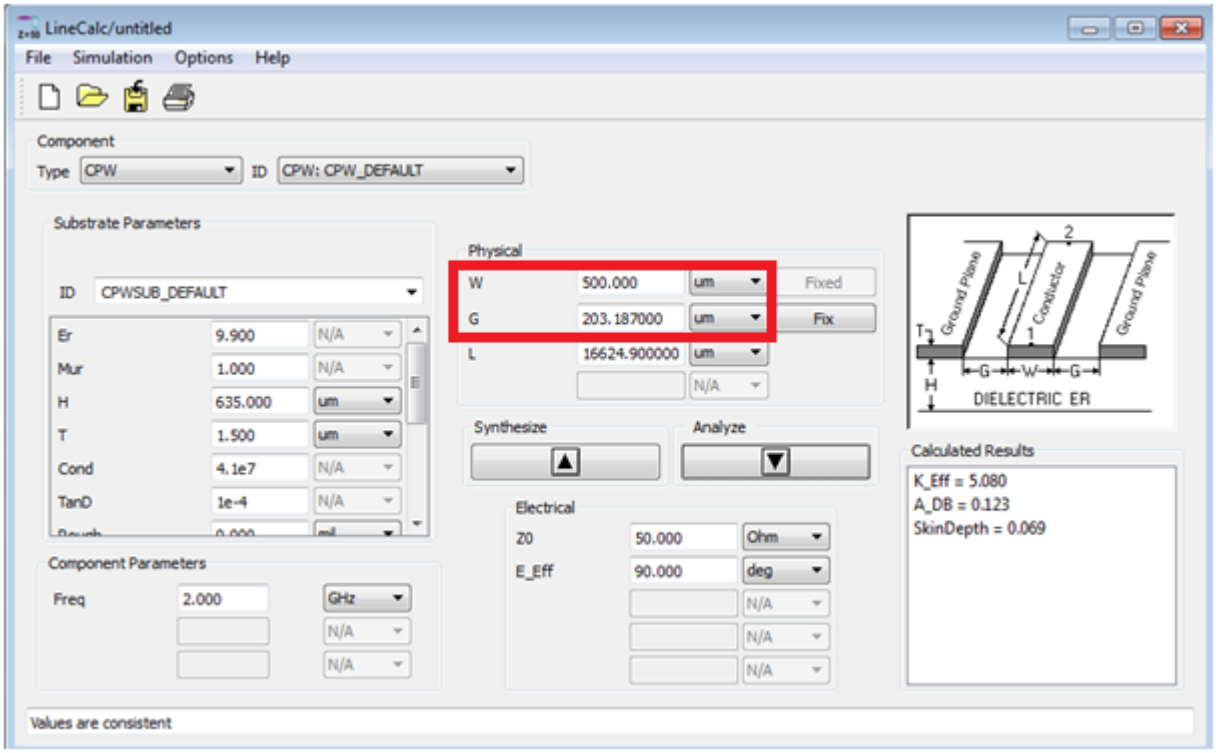

Figure 4.9: CPW dimensions: width of the signal line and its corresponding gap

The circuit is to be printed on an Alumina substrate with a thickness of 635 μm and using a gold metalization with a thickness of 2.5 μm. All these characteristics are presented in detail in Figure 4.10.

This being said, the Sonnet layout of such a CPW line is simulated and its characteristic impedance is analyzed.
In order to obtain this characteristic impedance Eq. 4.1 is used and further plotted over frequency as shown in Figure 4.11 (b).

$$Z_c = 50 * \sqrt{\frac{(1+S_{11})^2 - S21^2}{(1-S_{11})^2 - S21^2}} \tag{4.1}$$

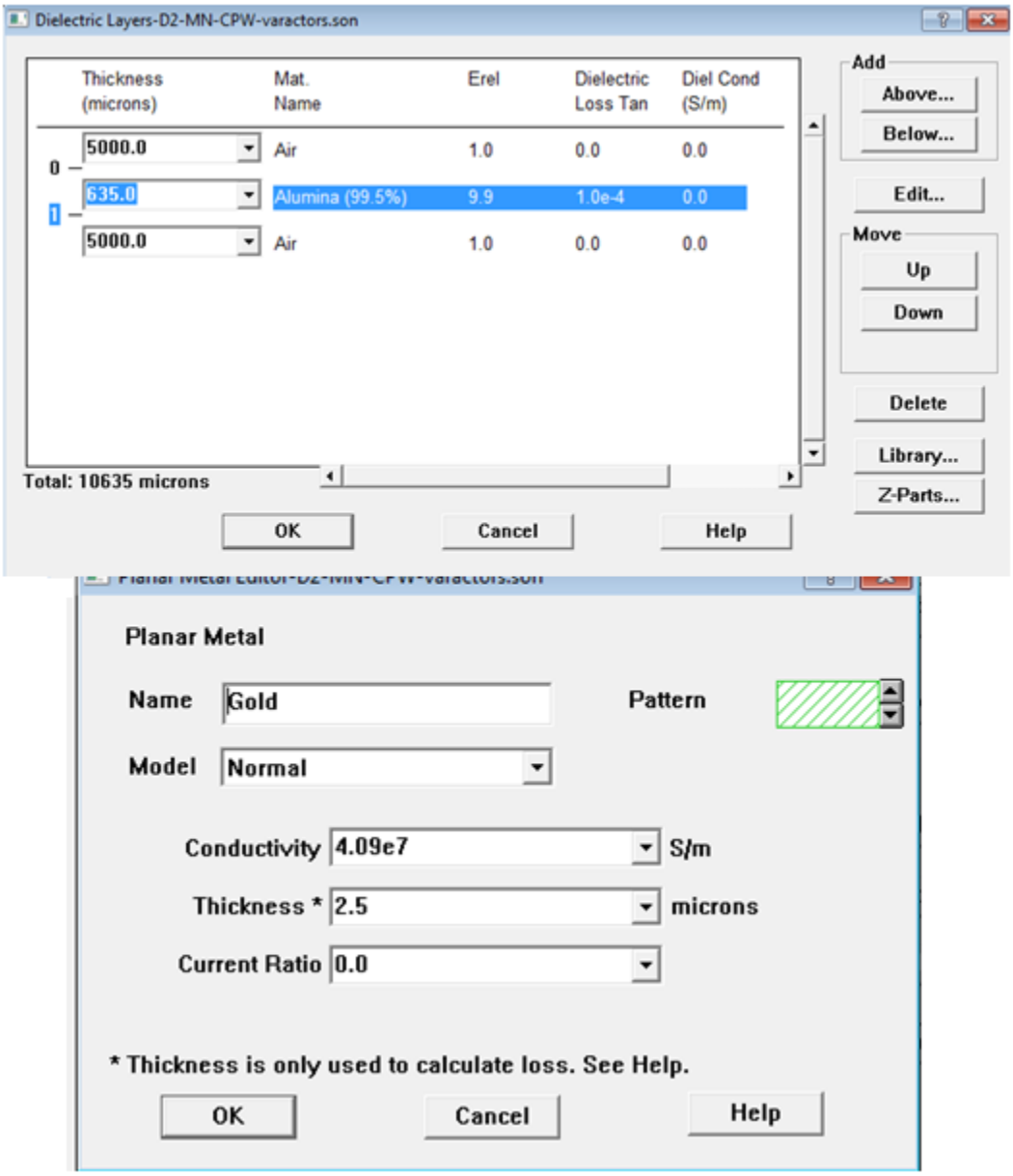

Figure 4.10: Substrate and Metalization characteristics

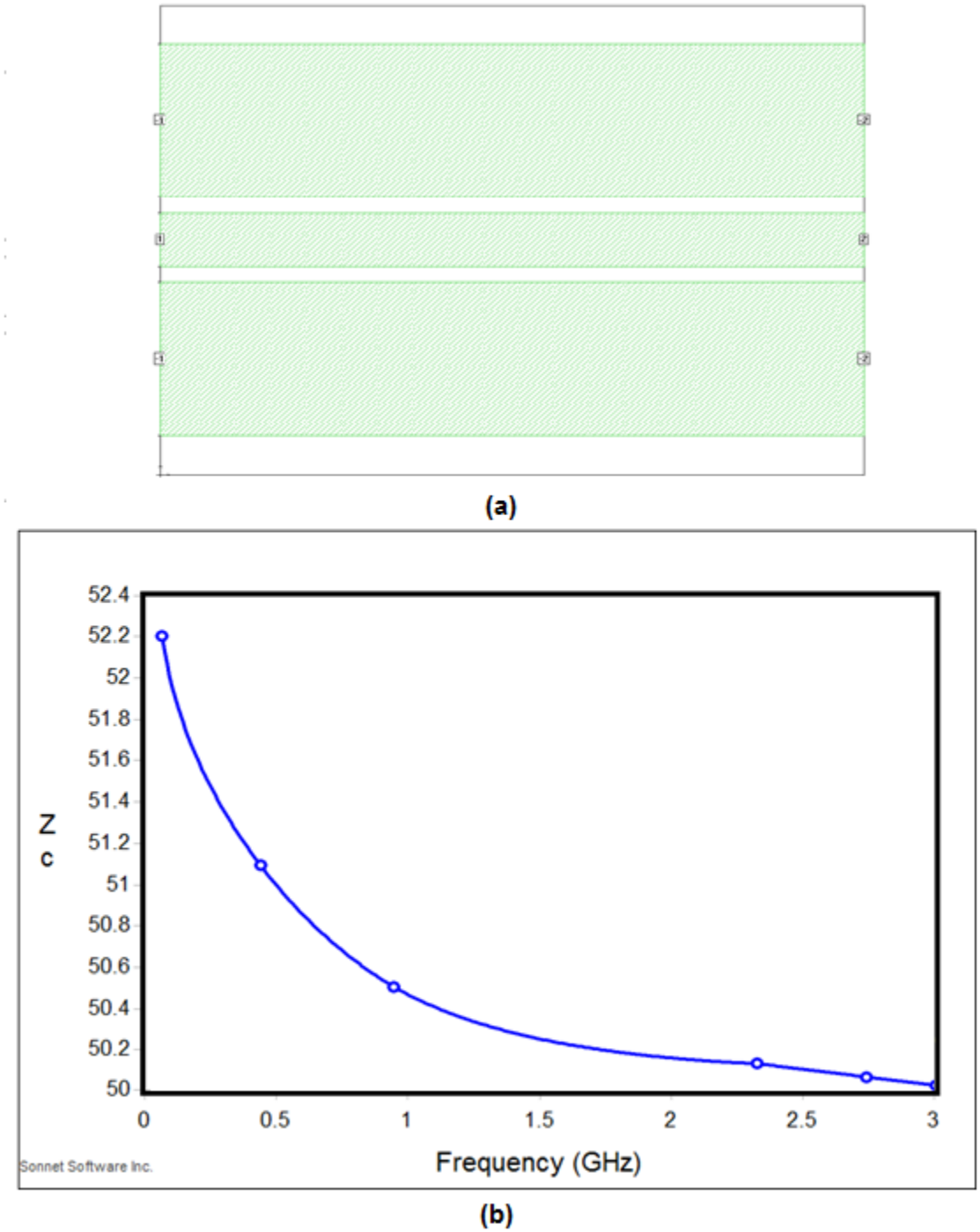

Figure 4.11: CPW transmission line: (a) Layout and (b) Characteristic impedance

At this point, the dimensions of the CPW, giving 50 Ω characteristic impedance, that is going to be used for all the circuit designs, are as follows:

- Width of the signal line: W=500 μm;
- Gap between the signal line and the ground plane: G=200 μm.

It is now possible to proceed to the next step: the design of the switch-capacitor bank. Several sets of simulations are held in this sense, so that the optimum design is found. A first option was to have the structure shown in Figure 4.12, where the switches would be positioned on the bottom ground plane of the CPW, aligned next to each other.

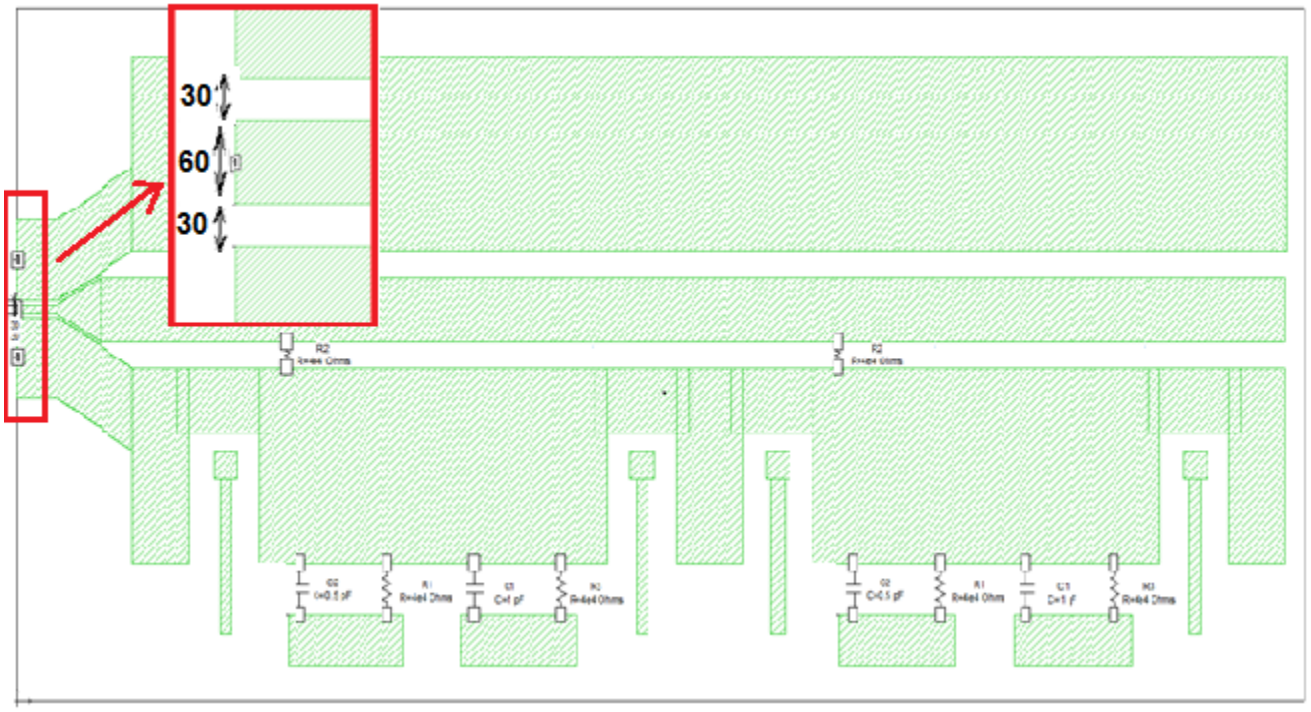

Figure 4.12: Initial Sonnet layout of the 16-state switch-capacitor bank

It is easily noticeable that this implies a rather long structure that is in contradiction with our goal of having the smallest possible sizes.

For measurement purposes, the input of the CPW line must be able to accommodate the 150 μm pitch ground-signal-ground of the coplanar RF probes, so W and G must be adjusted as follows, while still providing a 50 Ω characteristic impedance:

- Width of the signal line: W=60 μm;
- Gap between the signal line and the ground plane: G=30 μm.

The dimensions of the CPW transmission line are summarized in Table 4.1.

Table 4.1: Dimensions of the CPW Transmission Line

	Width of the signal line [um]	**Gap [um]**
CPW	500	200
Tapering	60	30

Due to its unsatisfactory size, the design must be changed so that more reasonable dimensions are achieved.

The switches are to be positioned as follows: one on each ground plane of the CPW, not next to each other anymore.
As a result the size of the layout is reduced to half of the previous one.

This final structure, that is to be fabricated, is shown in Figure 4.13. Its dimensions are 6200 x 5500 microns.

The manufacturer of these Radant switches is providing s2p files[1]containing measurements results for each state of the switch, allowing for a detailed analysis of the 16 possible states that the capacitor bank is offering.

[1] s2p file is a Touchstone file format used for documenting the data of a 2-port network. Most commonly, the S-parameters of such networks are recorded.

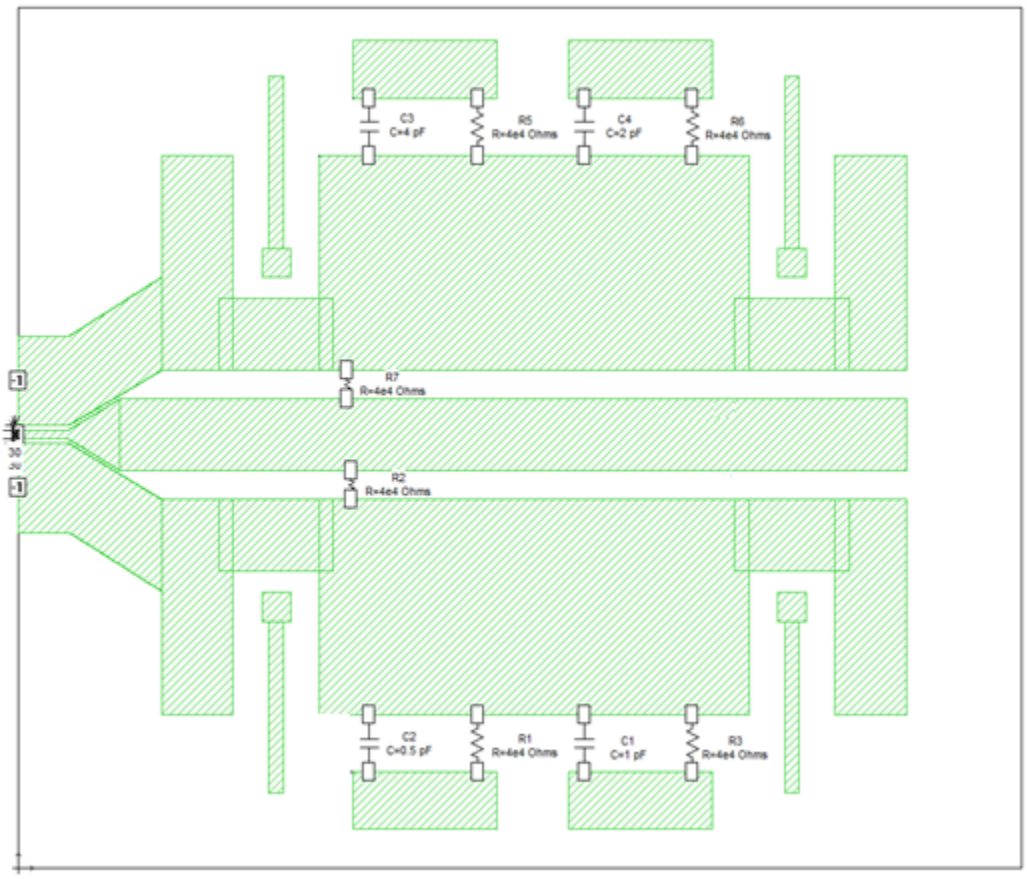

Figure 4.13: Final Sonnet layout of the 16-state switch-capacitor bank

Figure 4.14 shows the 16 states of the simulated capacitor bank. The obtained results meet the expectations: a minimum capacitance is achieved for the OFF state, when all four branches of the switch are disconnected, and a maximum value is achieved for the ON state of both switches. This is for a later comparison with the measuremnt results of the fabricated circuit.

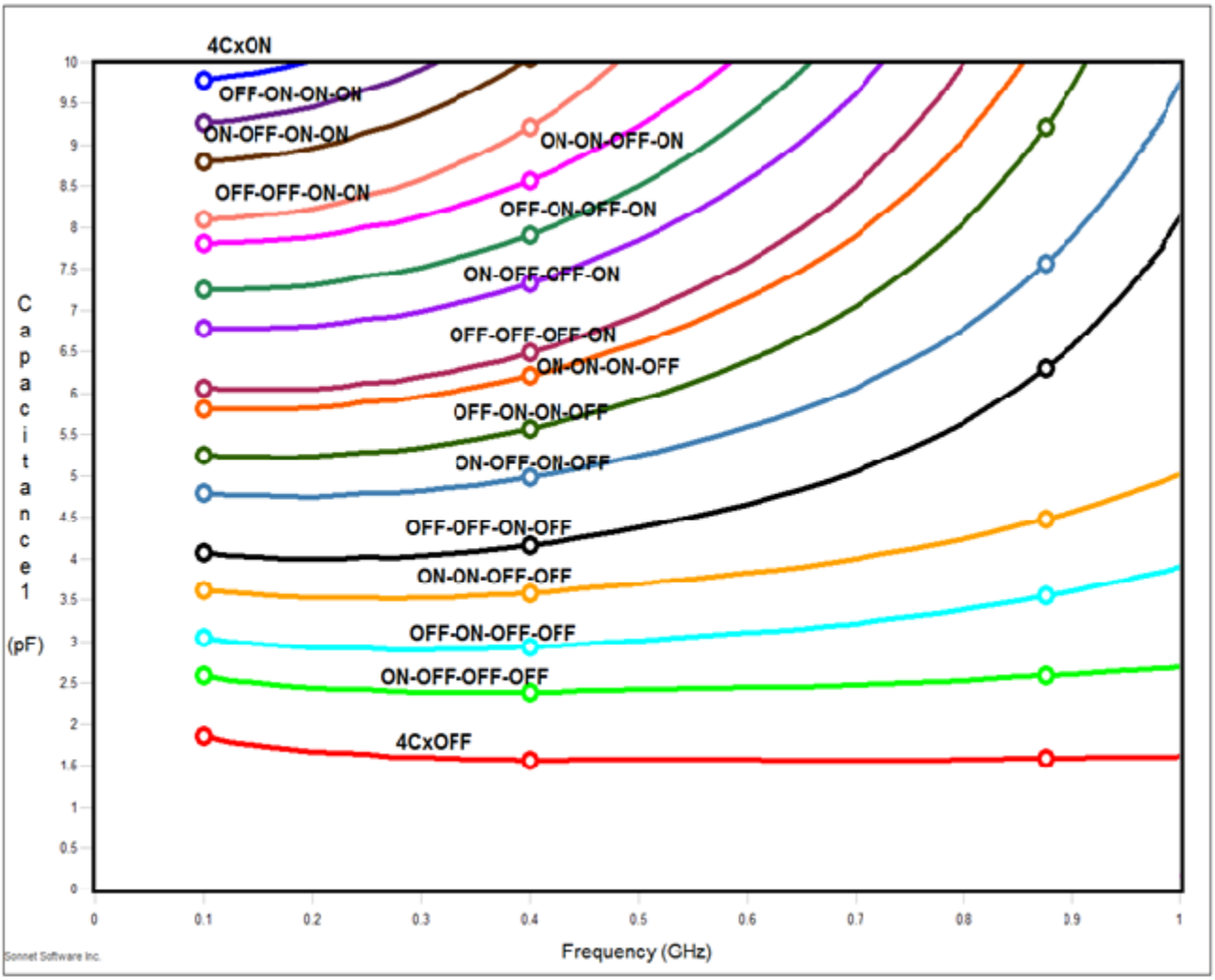

Figure 4.14: SONNET layout: Capacitance of the 16-state switch-capacitor bank

4.3.2 Measurements of the Fabricated Capacitor Bank

Once the layout is finalized, the next step is printing its mask and further fabricating it in the CIRFE cleanroom. As a result, the structure shown in Figure 4.15 is obtained.

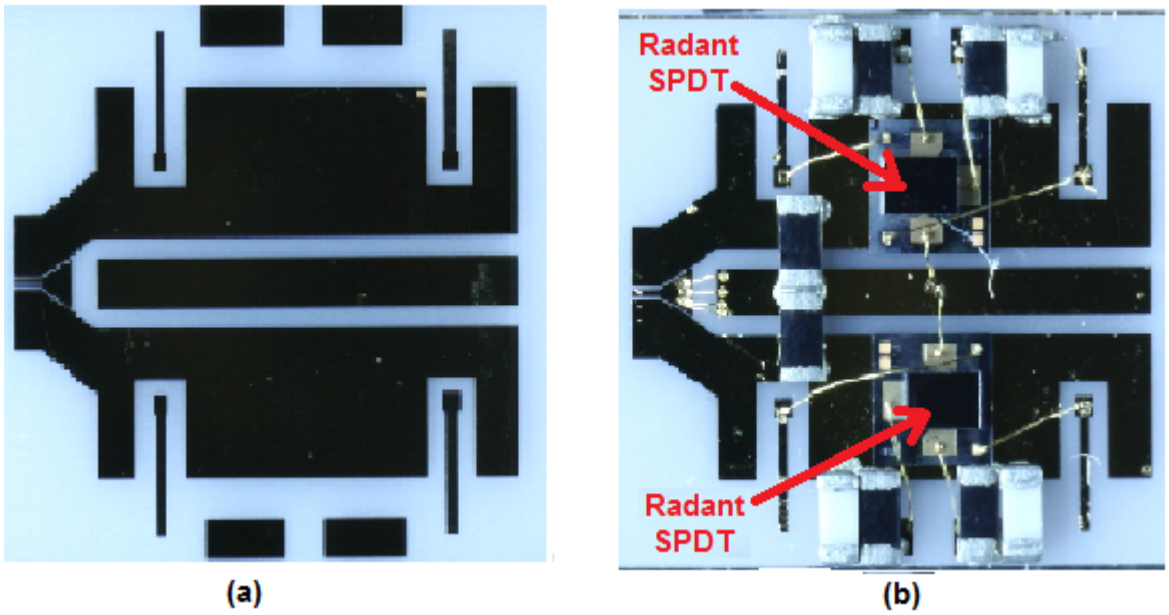

Figure 4.15: Fabricated switch-capacitor bank: (a) empty sample and (b) sample with the components assembled

In order to measure this structure, an RF signal is applied on the CPW line and a voltage on the DC pads so that the switches will be actuated. The actuation voltage in this case is around 80V. The measurement results of the circuit shown in Figure 4.15 (b) for the 16 combinations corresponding to the 16 states are presented in Figure 4.16.

From the plot it can be noticed that at the Cellular GSM band of 850MHz, the capacitor bank is providing capacitance values varying from 1.6pF to 15pF. Depending on the application and on the frequency of interest, the capacitor bank circuit can be re-configured so that it meets any new requirements.

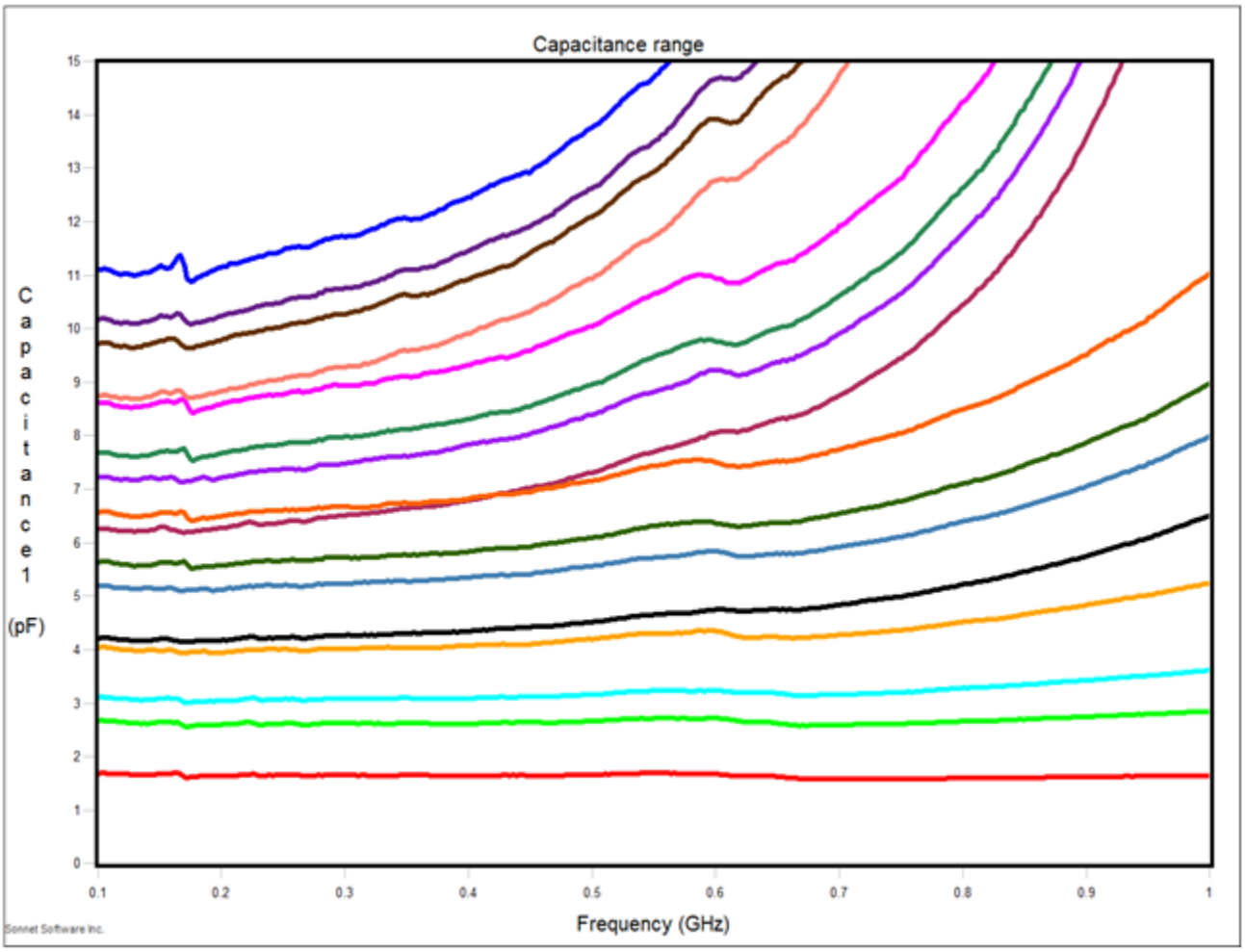

Figure 4.16: Measurement results of the fabricated circuit shown in Fig. 4.15 (b): Capacitance of the 16-state switched-capacitor bank

To appreciate the quality of the fabricated circuit, Figure 4.17 illustrates the differences between the simulation and measurement results of the capacitor bank. It can be noticed that the results are in good agreement. As expected, the actual fabricated circuit would provide higher capacitances, as an effect of the added wirebonds needed to assure the proper connections and that introduce extra capacitances.

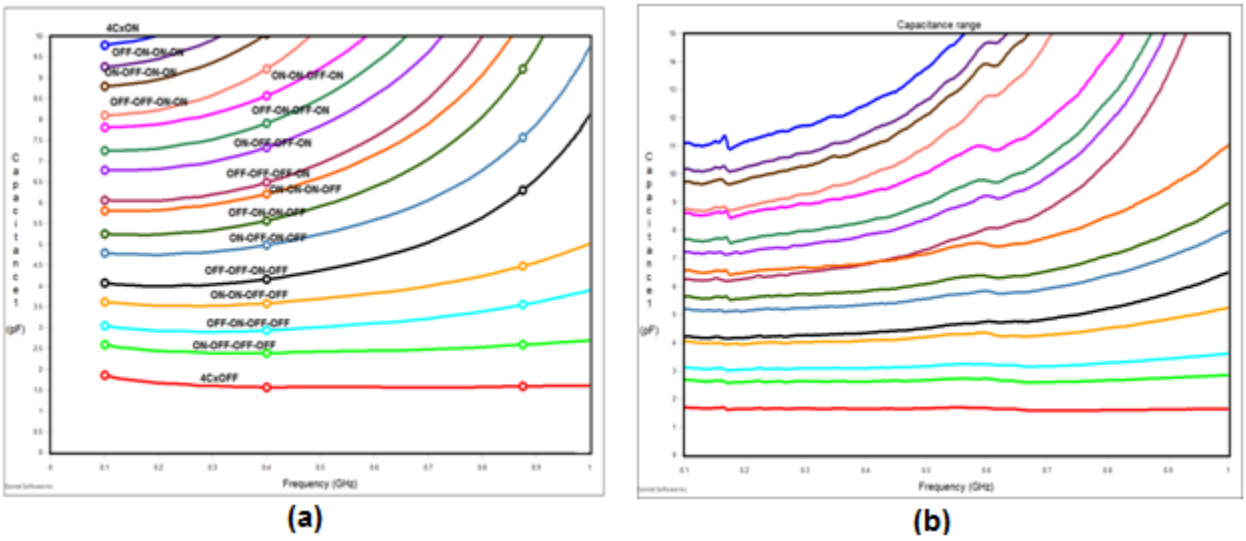

Figure 4.17: Comparison: (a) Simulation and (b) Measurement results of the 16-state switch-capacitor bank

4.3.3 Design and Simulation of a 4-state Switched-Capacitor Bank

For illustrative purposes only, the design of a 4-state capacitor bank is also proposed. The same Radant SPDT switch is to be used, although the design allows the assembly of SPST version as well, in series with two fixed capacitors, 0.5pF and 1pF. This circuit would be suitable for applications where a narrower capacitance range is needed. The simulations show that at a frequency of 850 MHZ, the capacitacne varies from 1.4pF to 4pF. Figure 4.18 shows both the Sonnet layout and the fabricated sample, along with the obtained capacitance ranges of the proposed 4-state capacitor bank.

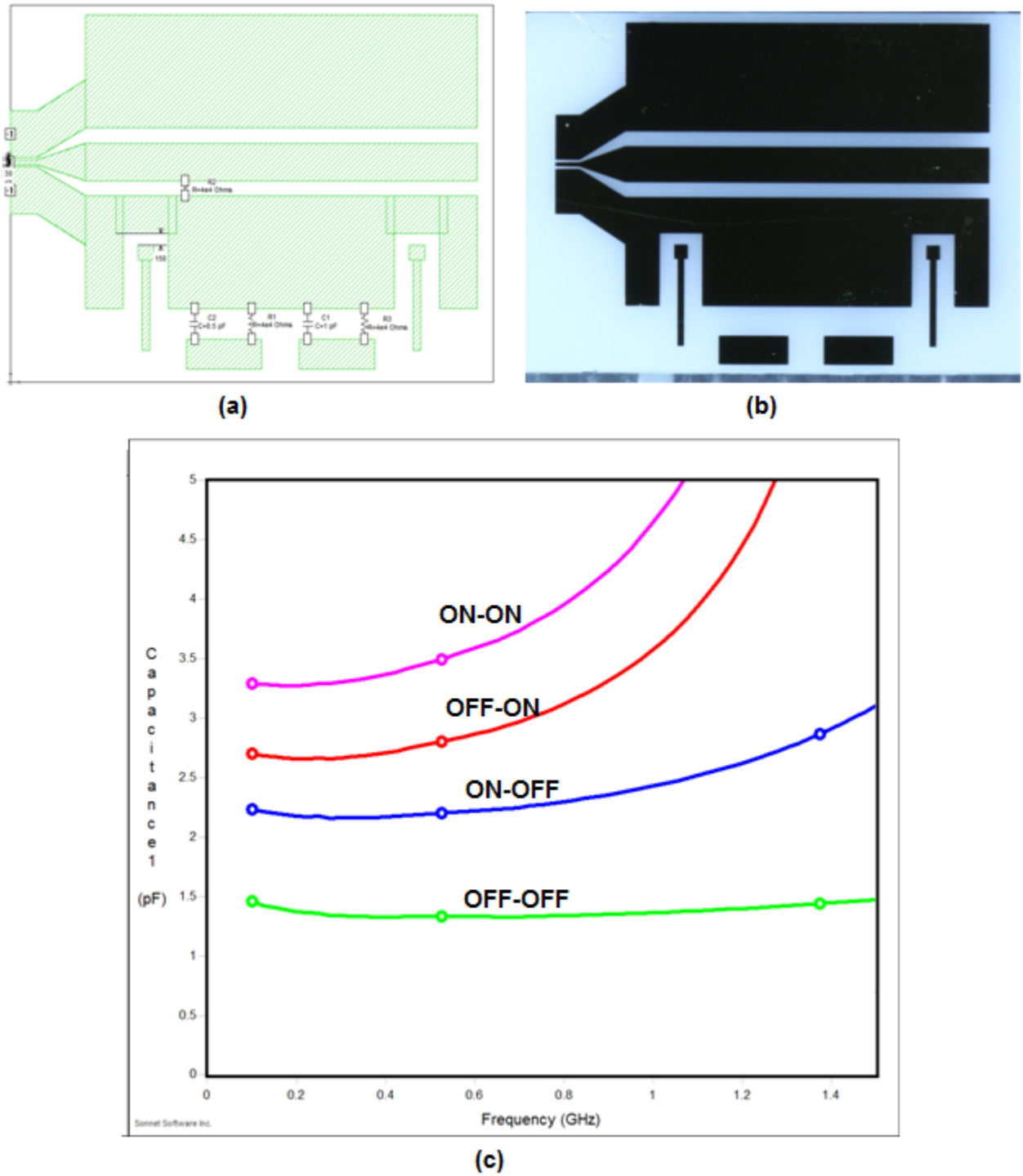

Figure 4.18: 4-state Capacitor Bank: (a) Layout, (b) Sample and (c) Capacitance range

4.4 Design of the Impedance Matching Network using the Switch-Capacitor Bank

It was earlier discussed that the low-pass Π-matching network topology is to be used as the base structure for the purpose of this thesis and that an inductor, L, and two capacitors, C, are needed as tuning elements. The 16-state capacitor bank presented in the previous section, and a commercial 2.2nH Taiyo Yuden inductor [52] shown in Figure 4.19, will play the role of the tuning elements.

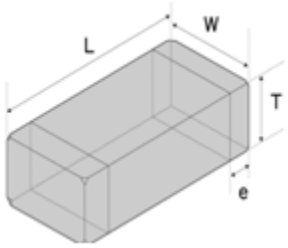

External Dimensions

L	1mm ±0.05
W	0.5mm ±0.05
H	0.5mm ±0.05
e	0.25mm ±0.10

Figure 4.19: Multilayer Chip Inductor - 0402 package dimensions [52]

4.4.1 Sonnet Layout Design and Simulation of the Impedance Matching Network

The same CPW that served for designing the capacitor bank, tapered so that it allows the positioning of the 150μm pitch ground-signal-ground coplanar RF probes, is used in this case as well. Several simulations are done in order to find the final layout of the network that meets all the requirements in terms of size, minimum wirebonds, while at the same time allowing safe and optimal placement of the chip components and Radant switches. Thus, a 2-port impedance matching network that takes all these into account is presented in Figure 4.20. Its dimensions are 10400 x 12000μm. It uses four Radant switches as part of the two capacitor banks, one inductor, eight fixed capacitors, two in series with each switch, and resistors that are necessary for the DC bias. As it can be noticed from

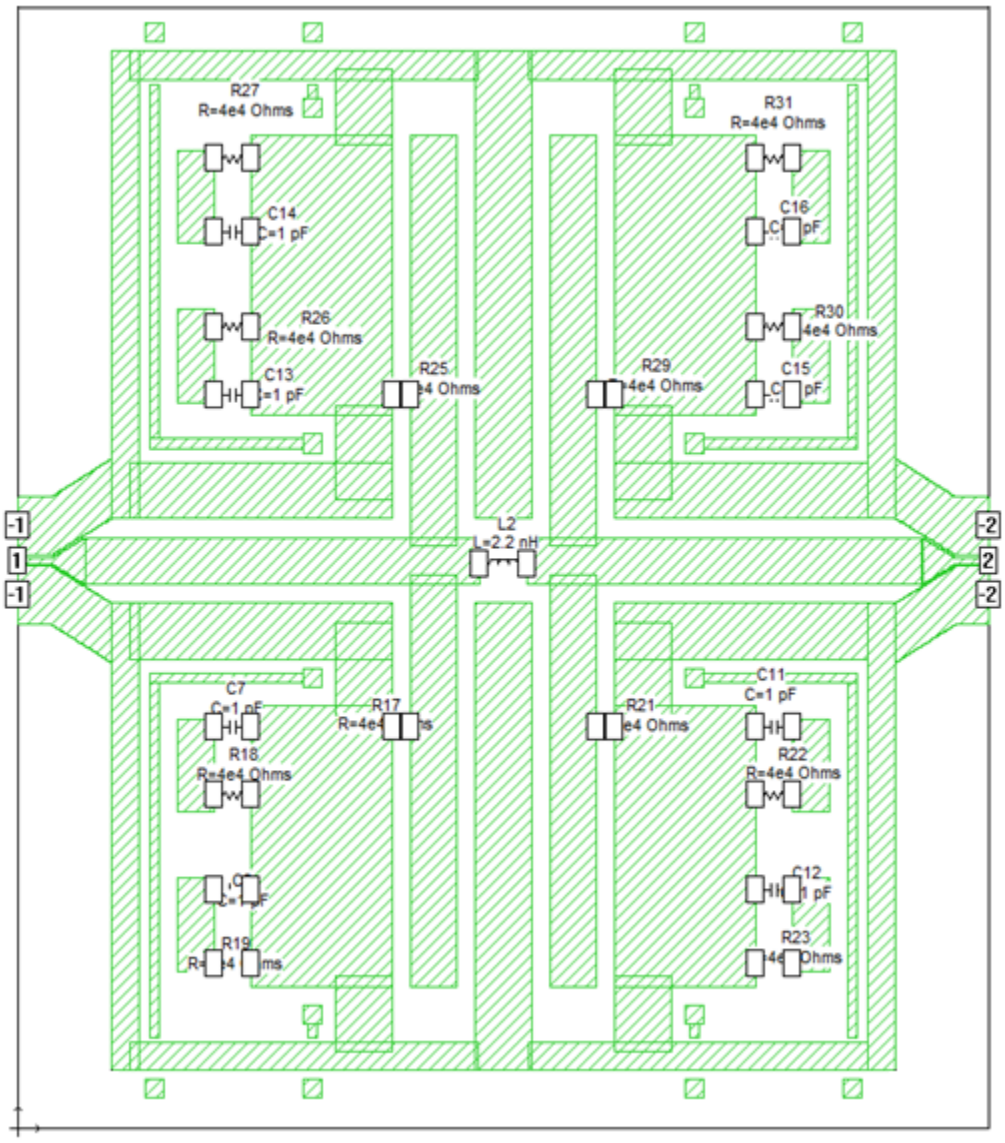

Figure 4.20: Sonnet layout of the Impedance Matching Network

this figure, the CPW signal line of the IMN is directly connected to the signal line of the capacitor bank, thus introducing a little gap in the ground plane of the CPW line. The effects of having this gap as a discontinuity in the ground plane are, in this case, minimal and would not affect the overall performance of the matching network due to the fact that the gap is much smaller than the wavelength λ (even much smaller than $\lambda/20$) so the 50 Ω impedance would still be achieved.

Regarding this designed impedance matching network, the point of interest is the dynamic range of the impedance that is to be analyzed on a Smith Chart as shown in Figure 4.21.

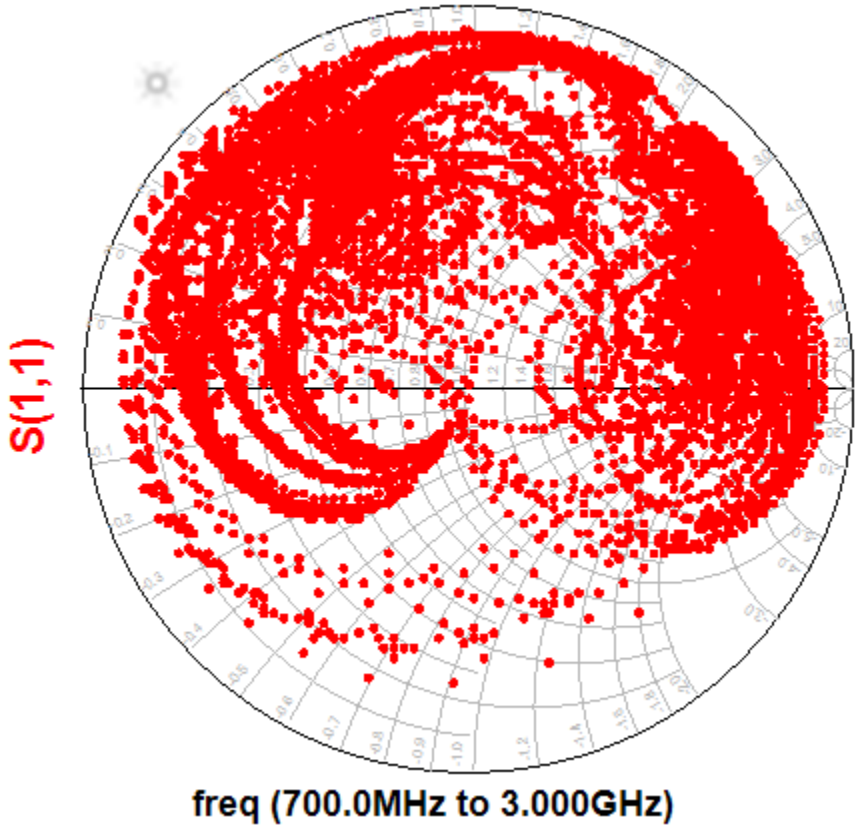

Figure 4.21: Simulated impedance dynamic range of the designed matching network using the supplied data files for the switches

As it can be seen, the matching network assures good coverage on the Smith Chart meaning that all these impedances can be perfectly matched to 50 Ω.

As previously mentioned, the gap introduced in the ground plane of the CPW line may have a certain influence on the performance of the IMN. Concerning this aspect, a second IMN is designed, as shown in Figure 4.22, where the ground plane does not have any discontinuity and where wirebonding would be necessary in order to connect the signal line of the IMN to the signal line of the capacitor bank. As in the previous design, it is preferred that the DC pads be placed on the top and bottom edges of the circuit, as indicated by the red arrows in the figure. In order to illustrate the notion of wirebonding, Sonnet offers the possibility of using via holes to create a "bridge-like" connection as shown in the figure.
Similar to the previous design, (Fig. 4.20), the impedance dynamic range is analyzed and it is concluded that there is no significant difference in terms of Smith Chart coverage between the two proposed structures. However, in order to minimize the effects introduced by wirebonds, it is decided to proceed with the first proposed design where the signal line is continuous.

For comparison purposes only, and to emphasize the importance of using the switch-capacitor bank, another impedance matching network is simulated using ADS circuit simulator. Instead of the capacitor bank, two variable capacitors are used, whose values are swept accordingly, following the capacitance ranges of the previously designed capacitor bank. This approach is presented in Figure 4.23 where it is easily noticeable that the Smith Chart coverage is not as good as in the previous case, thus proving the efficiency and higher performance of the capacitor bank compared to variable capacitors.

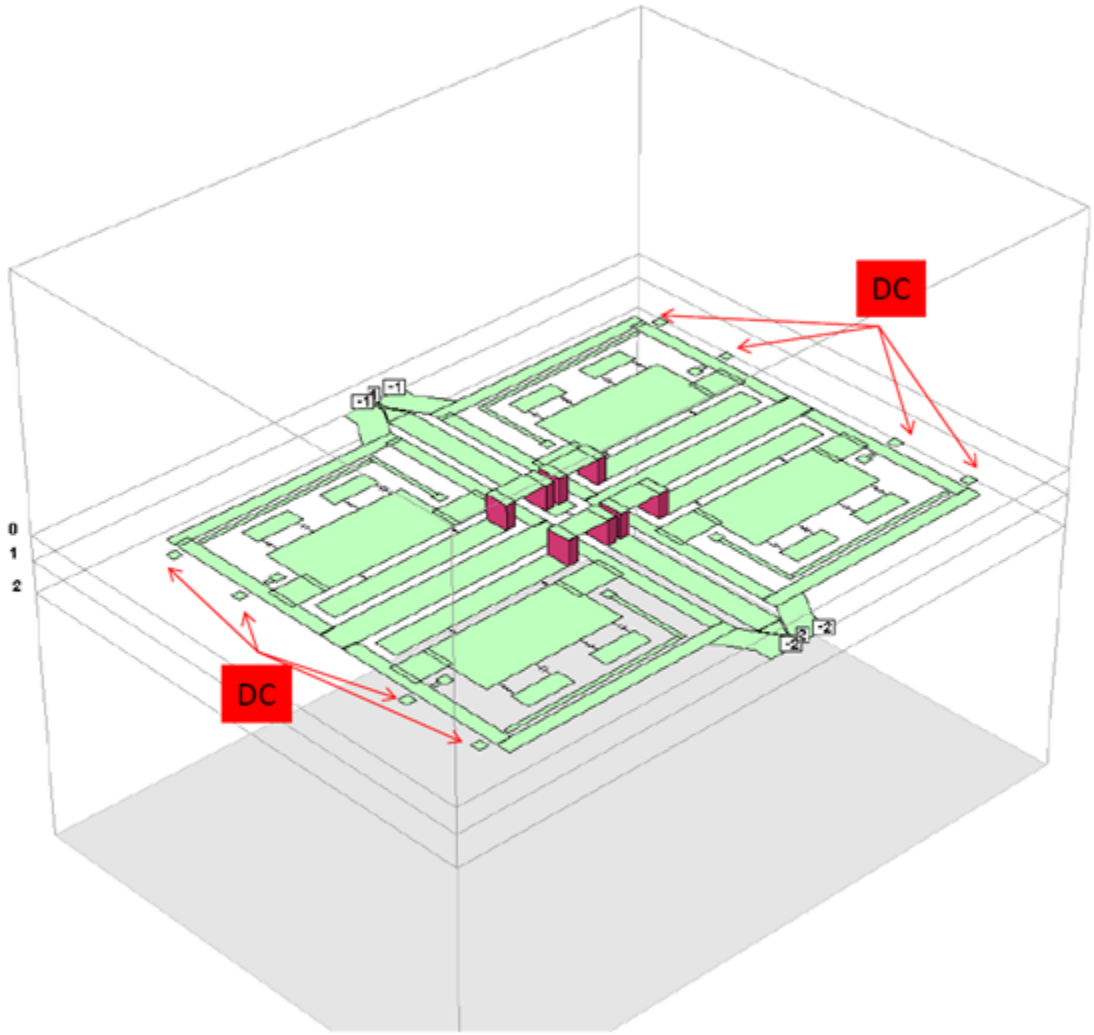

Figure 4.22: Sonnet 3D view of a second design of the Impedance Matching Network

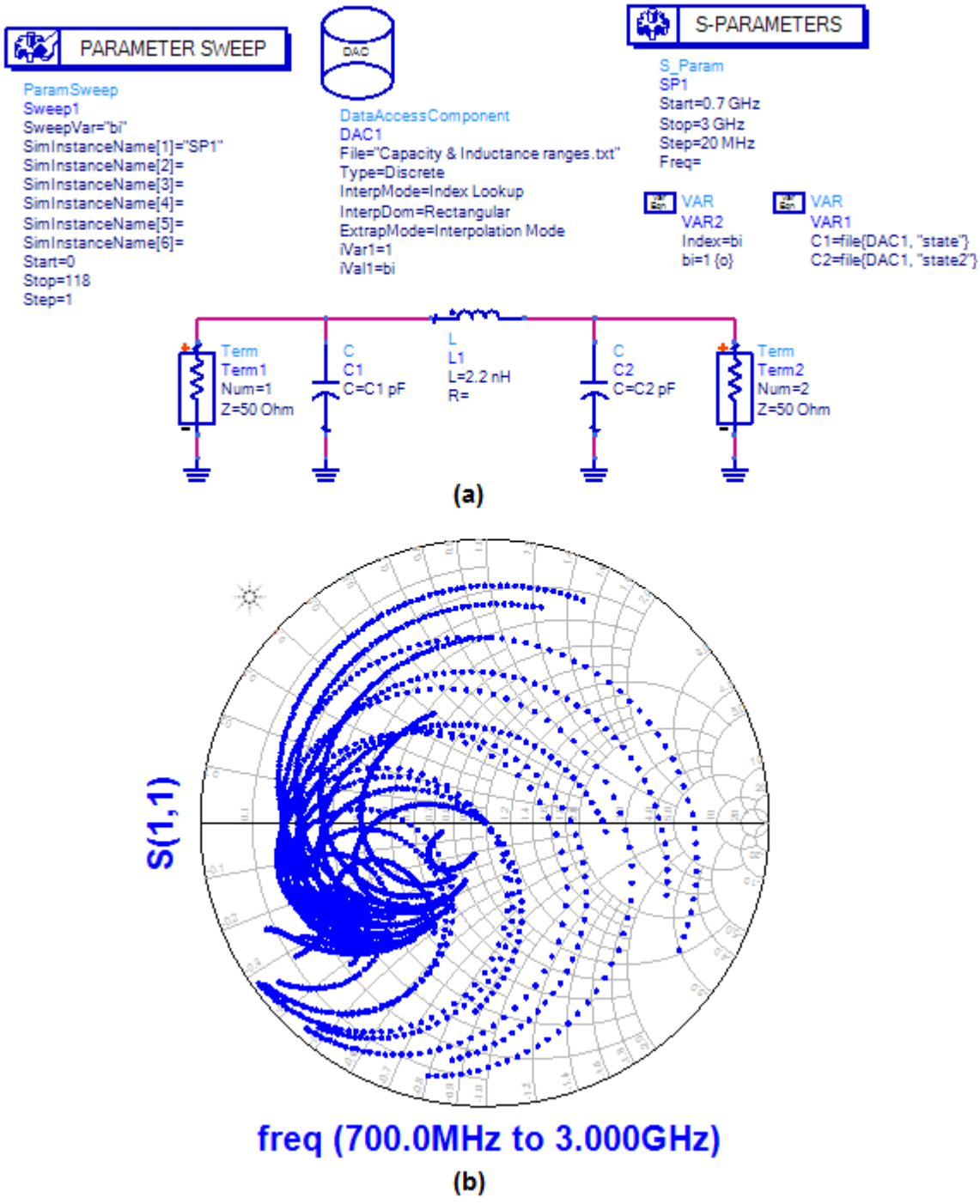

Figure 4.23: Impedance Matching Network using varactors with a limited capacitance range of 1-7 pF: (a) Circuit design and (b) Dynamic range of the impedance

Next, the focus is on the fabrication and measurement results of the impedance matching network described in Figure 4.20.

4.4.2 Fabrication and Measurement of the Impedance Matching Network

The same procedure as for the capacitor bank is followed in this case as well. The layout is sent for printing a mask that is used for the circuit fabrication in the CIRFE cleanroom leading to the impedance matching network shown in Figure 4.24.

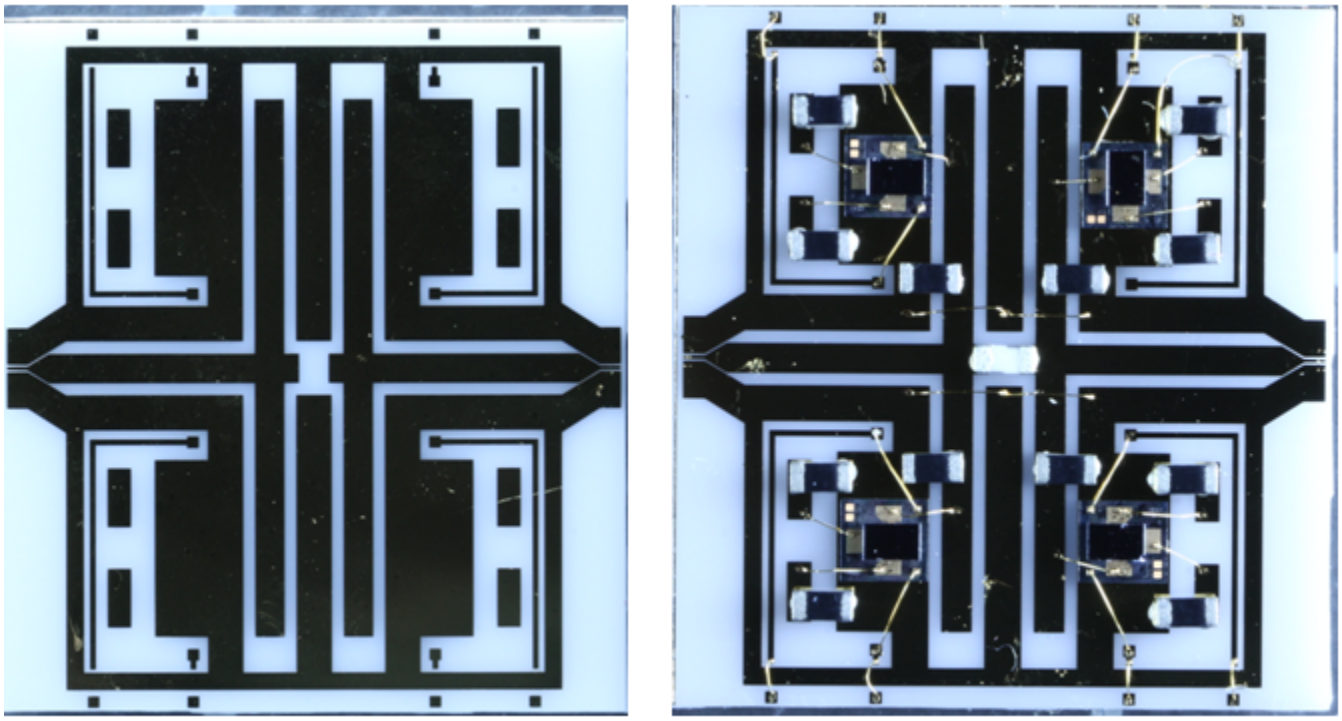

Figure 4.24: Fabricated Impedance Matching Network: (a) Empty sample and (b) Sample with the components assembled

Once the assembly is done, the circuit is measured after applying the proper DC actuation voltage for the MEMS switches and RF signal for the CPW line. Taking into account that this structure is using two capacitor banks, there are 16^2 possible combinations of states that will assure a wide range of impedances being matched to 50 Ω. In order to show this range, the Smith Chart is again used to plot the reflection coefficient, S_{11} as shown in Figure 4.25.

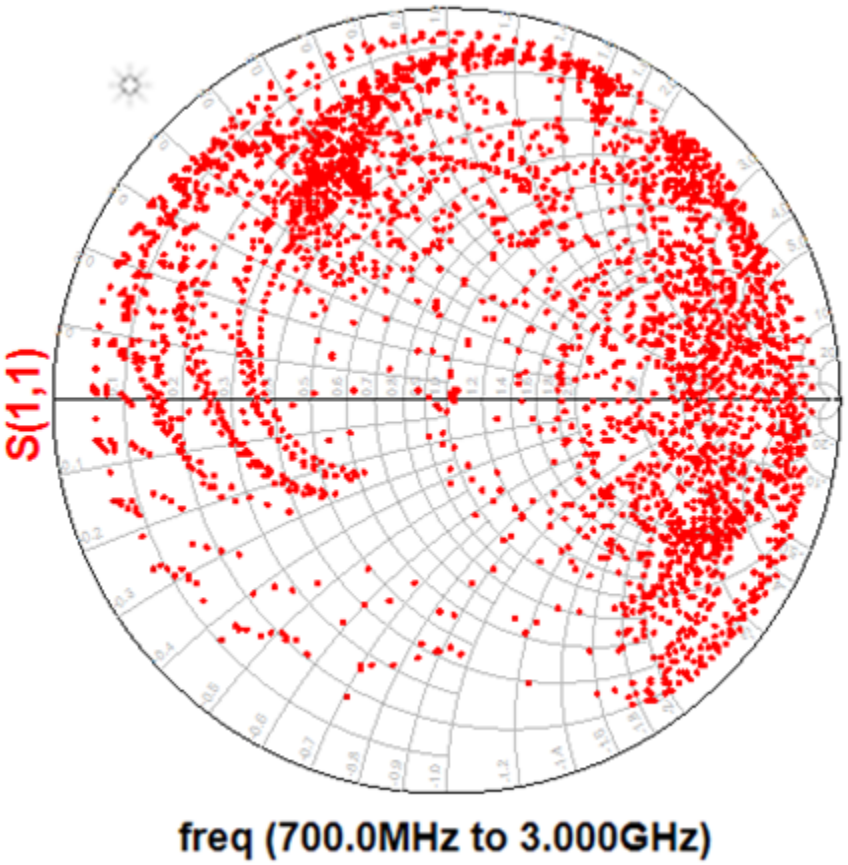

Figure 4.25: Measured impedance dynamic range of the fabricated matching network

It is noticeable that the measurements are in good agreement with the simulations, thus proving the performance that is expected from the fabricated IMN. Slight differences appear due to the effects introduced by the wirebonds and components parasitics.

4.5 Fabrication process

The impedance matching network, as well as all the circuits designed for the purpose of this thesis are fabricated at University of Waterloo, in the CIRFE lab, as part of the UW-MEMS process.
All the steps of the fabrication process are presented in Figure 4.26 where the so-called "through-mask electroplating" is implemented. To start with, as step 0, it is necessary to clean the wafer so that any possible contamination is removed. This is achieved through RCA-1 clean which is a wet chemical treatment. Once this is done, the procedure is as follows:

1. A 50nm chromium (Cr) adhesion layer and 50 nm gold (Au) seed layer are deposited on a 635 μm Alumina substrate with a dielectric constant of 9.9 and loss tangent of 2e-4.

2. Using the printed Light Field (LF) mask[2], containing the desired pattern, negative photoresist[3] is patterned, exposed to UV and then developed. Thus, the mold for the electroplating is prepared.

3. The CPW metalization lines are formed by electroplating 2 μm of gold (Au) in the electroplating bath

4. Evaporate 30 nm of Cr for the lift-off process

5. Kwik Strip is to be used in order to perform the lift-off of the photoresist in the mold

6. Etch away the gold seed layer using a wet etchant

7. Since Cr was used both as adhesion layer and for the lift-off process the etching can now be done in one step and the final structure is obtained. The etching should

[2]In a LF mask Chromium protects the portion where the structure is to be designed

[3]AZ NLOF 2035 is the negative resist used in this case. Its negative feature means that after UV exposure and development, the exposed resist remains. This type of resist is well-suited for lift-off and for any other processes where resist structures with high to very high thermal stability are required.

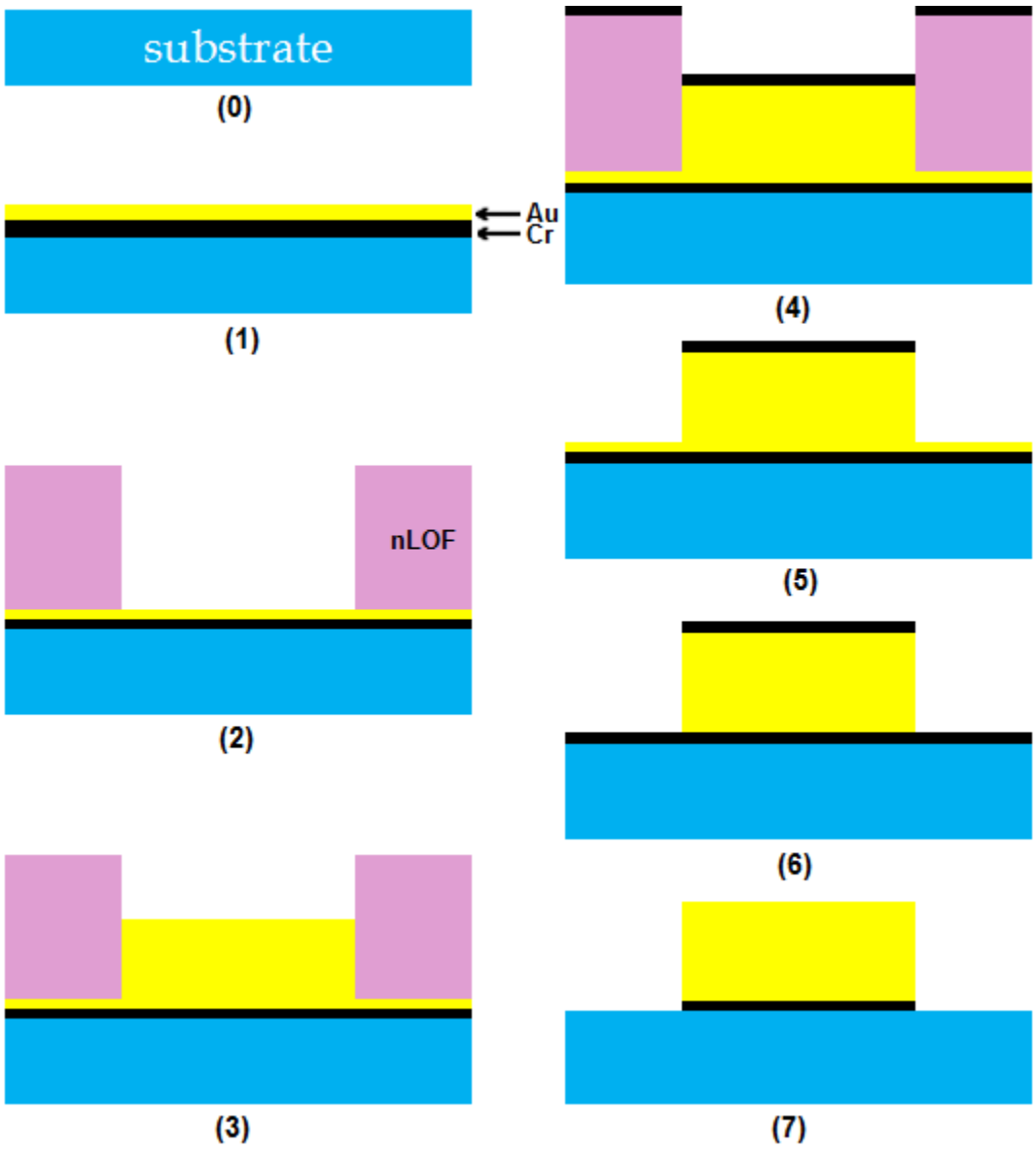

Figure 4.26: Steps of the fabrication process

be timed carefully in order not to underetch too much the adhesion layer and thus resulting in the peeling off of the gold structures.

As a result, the wafer illustrated in Figure 4.27, is fabricated to have several copies of the impedance matching networks and capacitor banks discussed in this chapter. When diced, the circuits are separated in individual samples that are further assembled and measured as shown in the previous sections.

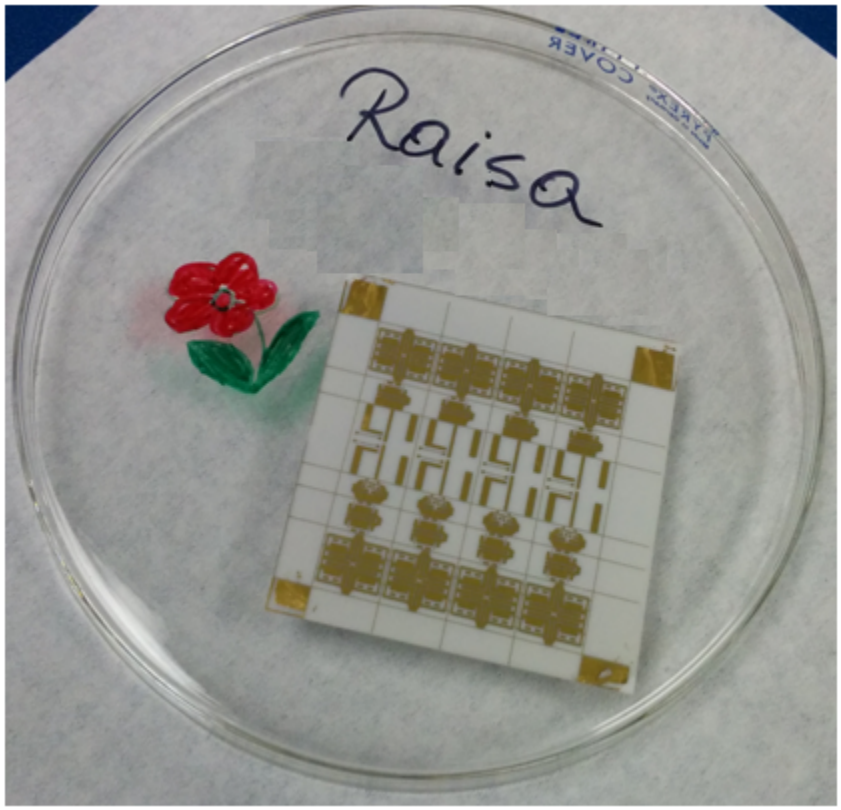

Figure 4.27: Printed circuits on an Alumina substrate

4.6 Summary

Design, simulation, fabrication and measurement results of different tuning elements and impedance matching networks were presented and analyzed in detail in this chapter.

Firstly, careful attention is paid to choosing the appropriate topology for the IMN that is to be designed. In this sense, it is decided that the low-pass Π-network is the most suitable, due to its ability of matching wide impedance ranges and to the fact that it is easy and convenient to implement by only using one fixed inductor and the two variable capacitors as tuning elements.

Further, the tuning elements are considered. A 16-state switch-capacitor bank, using two SPDT Radant switches is discussed in this context. Also, a 4-state capacitor bank is proposed for applications where a smaller capacitance range is needed.

With these well-defined tuning elements the matching network is to be designed. Two impedance matching network layouts are presented along with a comparison between IMN using switched-capacitor bank and IMN using conventional variable capacitors.

At the end, it is proven that the fabricated network offers satisfactory performance, a wide range of impedance is covered on the Smith Chart, and the measurement results are in good agreement with the simulations. It can be said that a wider Smith Chart coverage could possibly be achieved with a capacitor bank that uses more MEMS Radant switches.

All the circuits fabricated for the purpose of this thesis are presented in Figure 4.28, next to a 25cents coin, for a better size estimation. Their dimensions are also summarized in Table 4.2.

Table 4.2: Dimensions of the Fabricated Circuits

Fabricated Circuit	**Dimensions [mm]**
16-state switched-capacitor bank	6.2 x 5.5
4-state switched-capacitor bank	6.2 x 5.5
Impedance matching network	10.4 x 12

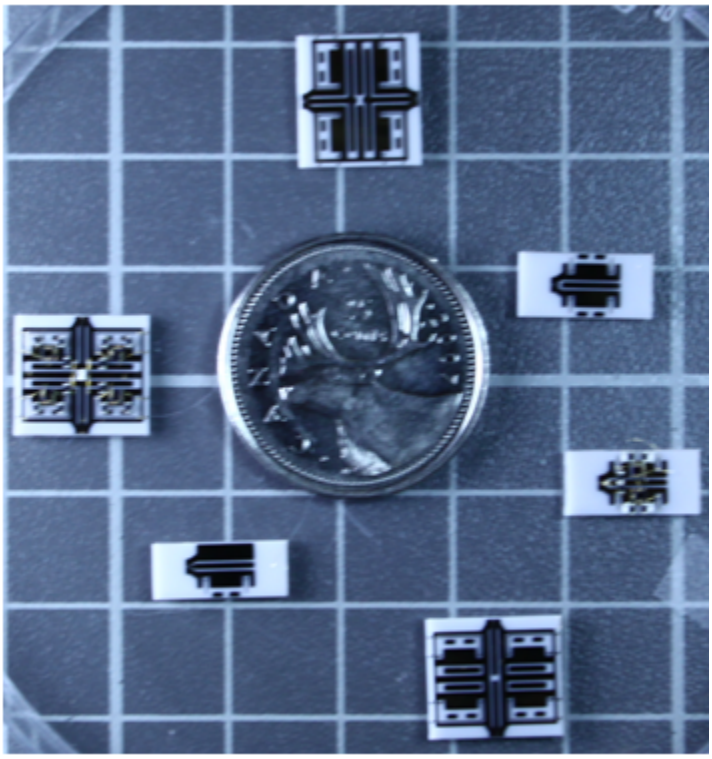

Figure 4.28: Different Fabricated Devices compared to a 25 cents coin

Chapter 5

Conclusion

The main focus of the present thesis is on the design, simulation, fabrication and measurement of RF impedance matching networks designated for wireless applications. Particular interest is given to their tuning elements that are thoroughly analyzed. The contributions brought to this topic along with proposed future work are outlined in this chapter.

5.1 Contributions

The main contributions brought along with this thesis can be summarized as follows:

- Initially, a detailed analysis is carried out addressing the feasibility of switch-capacitor banks using different types of RF switches. RF switches, used for tuning, are preferred over the traditional varactors due to their high performance in terms of linearity, low losses, and high power handling. Three types of switches are discussed and further simulated when connected in series with fixed capacitors. In this way switched-capacitor banks are built, so that based on the state of the switch, different variable capacitance values are achieved.

- Once this step is finished, it is necessary to make a decision regarding the structure of the impedance matching network. In this sense, several network topologies

are analyzed, each one of them presenting unique features, suitable for a variety of applications. Careful analysis is required in order to choose the most suitable one. As a result, the low-pass Π network topology is selected as the best candidate for the present work. This topology allows wide impedance tuning ranges, it is easy to implement and commonly used in the literature.

- Next, the design and EM simulation of the switched-capacitor banks are presented. This design is based on well-established microwave methods that have been adapted and developed to continuously improve the tuning properties of the devices and allow reconfiguration for different load conditions and impedances. CPW transmission lines are used for the RF signal transmission and Sonnet software is used in this case for drawing the capacitor bank layout and for all the EM simulations.

- The above mentioned capacitor bank is implemented in the structure of the impedance matching network and the entire design process is presented. Several sets of simulations are held until defining the final layout of the network. Important factors such as the final dimensions of the circuit and length of the wirebonds needed for the connections with the board, are taken into consideration in this sense.

- Both the switched-capacitor bank and the impedance matching network are fabricated in the CIRFE lab at UW as part of UW-MEMS process, on Alumina substrate and employing Radant MEMS switches.

- The impedance matching network is then measured and the results show good matching over a wide frequency range, 700 MHz - 3 GHz, suitable for wireless applications. A comparison between matching networks using RF MEMS switches and matching networks using conventional varactors is also carried out. The performance is shown in terms of Smith Chart coverage, and as expected, the RF MEMS approach demonstrates a better RF performance.

5.2 Future Work

In terms of future plans concerning this topic there are several aspects worthy of exploration in the coming period:

- Further investigation in terms of life time and reliability of the proposed MEMS-based Impedance Matching Network.
- Also, it is important to test the network at high power and analyze its behavior in these conditions.
- The tuning speed of the network must be also investigated since this may become an undesired parameter.
- Finally, it would be interesting to see the performance that can be achieved by the network using different types of switches, such as Peregrine or Omron.

APPENDICES

Appendix A

List of Acronyms

IMN	Impedance Matching Networks
ATU	Antenna Tuning Units
RF	Radio Frequency
MEMS	MicroElectroMechanical Systems
SOI	Silicon-On-Insulator
BST	Barium Strontium Titanate
SPST	Single Pole Single Throw
SPDT	Single Pole Double Throw
CMOS	Complementary Metal Oxide Semiconductor
GSM	Global System for Mobile Communications
CDMA	Code Division Multiple Access
WLAN	Wireless Local Area Network
EM	ElectroMagnetic

References

[1] J. de Mingo, A. Valdovinos, A. Crespo, D. Navarro, and P. Garcia, "An RF Electronically Controlled Impedance Tuning Network Design and its Application to an Antenna Input Impedance Automatic Matching System," *IEEE Transactions on Microwave Theory and Techniques*, vol. 52, pp. 9–19, Feb. 2004.

[2] W. Neo, Y. Lin, X. Liu, L. de Vreede, L. Larson, M. Spirito, M. Pelk, K. Buisman, A. Akhnoukh, A. de Graauw, and L. Nanver, "Adaptive Multi-Band Multi-Mode Power Amplifier Using Integrated Varactor-Based Tunable Matching Networks," *IEEE Journal of Solid-State Circuits*, vol. 41, pp. 2166 – 2176, Sep. 2006.

[3] R. B. Whatley, Z. Zhou, and K. L. Melde, "Recongurable RF Impedance Tuner for Match Control in Broadband Wireless Devices," *IEEE Transactions on Antennas and Propagation*, vol. 54, pp. 470 – 478, Feb. 2006.

[4] I. C. Hunter and J. D. Rhodes, "Electronically Tunable Microwave Bandpass Filters," *IEEE Transactions on Microwave Theory and Techniques*, vol. 30, pp. 1361 – 1367, Sep. 1982.

[5] M. Makimoto and Z. Sagawa, "Varactor Tuned Bandpass Flters Using Microstrip-Line Ring Resonators," *IEEE Transactions on Microwave Theory and Techniques*, Jun. 1986.

[6] M. Nosrati and Z. Atlasbaf, "A New Miniaturized Electronically Tunable Bandpass FIlter," *7th International Symposium on Antennas, Propagation & EM Theory*, Oct. 2006.

[7] M. A. A. Latip, M. K. M. Salleh, and N. A. Wahab, "Tuning Circuit Based on Varactor for Tunable Filter," *IEEE International RF and Microwave Conference*, Dec. 2011.

[8] C. R. Trommer and L. Schmidt, "Bandpass Filter with Tunable Bandwidth and Center Frequency based on Varactor Diodes," *Proceedings of the 6th German Microwave Conference*, Mar. 2011.

[9] J. H. Sinsky and C. R. Westgate, "Design of an Electronically Tunable Microwave Impedance Transformer," *IEEE Transactions on Microwave Theory and Techniques*, vol. 2, pp. 647 – 650, Jun. 1997.

[10] J. Nath, D. Ghosh, J. Maria, A. I. Kingon, W. Fathelbab, P. D. Franzon, and M. B. Steer, "An Electronically Tunable Microstrip Bandpass Filter Using Thin-Film BariumStrontiumTitanate (BST) Varactors," *IEEE Transactions on Microwave Theory and Techniques*, vol. 53, Sep. 2005.

[11] H. Maune, M. Sazegar, and R. Jakoby, "Tunable Impedance Matching Networks for Agile RF Power Amplifiers," *IEEE MTT Microwave Symposium Digest*, Jun. 2011.

[12] O. Bengtsson, H. Maune, A. Wiens, S. A. Chevtchenko, R. Jakoby, and W. Heinrich, "RF-Power GaN Transistors with Tunable BST Pre-Matching," *IEEE MTT International Microwave Symposium Digest*, Jun. 2013.

[13] F. A. Miranda, C. H. Mueller, C. D. Cubbage, K. B. Bhasin, R. K. Singh, and S. D. Harkness, "HTS/Ferroelectric Thin Films for Tunable Microwave Components," *IEEE Transactions on Applied Superconductivity*, vol. 5, pp. 3191 – 3194, Jun. 1995.

[14] F. A. Miranda, G. Subramanyam, F. W. V. Keuls, R. R. Romanofsky, J. D. Warner, and C. H. Mueller, "Design and Development of Ferroelectric Tunable Microwave Components for Ku- and K-Band Satellite Communication Systems," *IEEE Transactions on Microwave Theory and Techniques*, vol. 48, pp. 1181 – 1189, Jul. 2000.

[15] B. H. Moeckly and Y. Zhang, "Strontium Titanate Thin Films for Tunable YBa2Cu3O7 Microwave Filters," *IEEE Transactions on Applied Superconductivity*, vol. 11, pp. 450 – 453, Mar. 2001.

[16] A. Tombak, F. T. Ayguavives, J. Maria, G. T. Stauf, A. I. Kingon, and A. Mortazawi, "Tunable RF Filters Using Thin Film Barium Strontium Titanate Based Capacitors," *IEEE MTT-S International Microwave Symposium Digest*, vol. 3, pp. 1453 – 1456, May 2001.

[17] A. Tombak, J. Maria, F. T. Ayguavives, Z. Jin, G. T. Stauf, A. I. Kingon, and A. Mortazawi, "Voltage-Controlled RF Filters Employing Thin-Film BariumStrontiumTitanate Tunable Capacitors," *IEEE Transactions on Microwave Theory and Techniques*, vol. 51, pp. 462 – 467, Feb. 2003.

[18] H. Maune, O. Bengtsson, F. Golden, M. Sazegar, R. Jakoby, and W. Heinrich, "Tunable RF GaN-Power Transistor Implementing Impedance Matching Networks Based on BST Thick Films," *Proceedings of the 7th European Microwave Integrated Circuits Conference*, Oct. 2012.

[19] Y. Shen, S. Ebadi, P. Wahid, and X. Gong, "Tunable and Flexible Barium Strontium Titanate (BST) Varactors on Liquid Crystal Polymer (LCP) Substrates," *IEEE MTT-S International Microwave Symposium Digest*, Jun. 2012.

[20] Chipworks, "Inside the BlackBerry Z10," Feb. 2013.

[21] A. van Bezooijen, M. A. de Jongh, C. Chanlo, L. Ruijs, F. van Straten, R. Mahmoudi, and A. van Roermund, "A GSM/EDGE/WCDMA Adaptive Series-LC Matching Network Using RF-MEMS Switches," *IEEE Journal of Solid-State Circuits*, vol. 43, pp. 2259 – 2268, Oct. 2008.

[22] J.Papapolymerou, K. Lange, C. Goldsmith, A. Malczewski, and J. Kleber, "Recongurable double-stub tuners using MEMS switches for intelligent RF front-ends," *IEEE Transactions on Microwave Theory and Techniques*, vol. 51, pp. 271 – 278, Jan. 2003.

[23] K. Lange, "A dynamically recongurable impedance tuner using RF MEMS switches," *M.S. thesis, Univ. Arizona, Dept. Elect. Comput. Eng., Tucson, AZ*, 2001.

[24] Y. Lu, D. Peroulis, S. Mohammadi, and L. Katehi, "A MEMS Recongurable Matching Network for a Class AB Amplier," *IEEE Microwave and Wireless Components Letters*, vol. 13, pp. 437 – 439, Oct. 2003.

[25] J. Brank, Z. J. Yao, M. Eberly, A. Malczewski, K. Varian, and C. L. Goldsmith, "RF MEMS-based tunable filters," *International Journal of RF and Microwave Computer-Aided Engineering*, vol. 11, pp. 276 – 284, Sep. 2001.

[26] C. L. Goldsmith, A. Malczewski, Z. J. Yao, and S. Chen, "RF MEMS variable capacitors for tunable lters," *International Journal of RF and Microwave Computer-Aided Engineering*, vol. 9, pp. 362 – 374, Jul. 1999.

[27] J. R. de Luis, A. Morris, Q. Gu, and F. de Flaviis, "Tunable Antenna Systems for Wireless Transceivers," *2011 IEEE International Symposium on Antennas and Propagation*, pp. 730 – 733, Jul. 2011.

[28] T. Viha-Heikkila, J. Vans, J. Tuovinen, and G. M. Rebeiz, "A Reconfigurable 6-20 GHz RF MEMS Impedance Tuner," *2004 IEEE MTT-S International Microwave Symposium Digest*, vol. 2, pp. 729 – 732, Jun. 2004.

[29] S. Fouladi, A. Akhavan, and R. R. Mansour, "A Novel Recongurable Impedance Matching Network Using DGS and MEMS Switches for Millimeter-wave Applications," *IEEE MTT-S International Microwave Symposium Digest*, pp. 145 – 148, Jun. 2008.

[30] F. Domingue, A. B. Kouki, and R. R. Mansour, "Tunable Microwave Amplifier Using a Compact MEMS Impedance Matching Network," *Proceedings of the 4th European Microwave Integrated Circuits Conference*, Sep. 2009.

[31] S. Fouladi, F. Domingue, N. Zahirovic, and R. R. Mansour, "Distributed MEMS Tunable Impedance-Matching Network Based on Suspended Slow-Wave Structure Fabricated in a Standard CMOS Technology," *IEEE Transactions on Microwave Theory and Techniques*, vol. 58, Apr. 2010.

[32] A. M. Mohamed, S. Boumaiza, and R. R. Mansour, "Novel Reconfigurable Fundamental/Harmonic Matching Network for Enhancing the Efficiency of Power Amplifiers," *Proceedings of the 40th European Microwave Conference*, Sep. 2010.

[33] G. M. Rebeiz, "RF MEMS for Wireless-Bands Tunable Networks," *IEEE Transactions on Microwave Theory and Techniques - Invited Talk*, June 2006.

[34] R. Mahameed and G. M. Rebeiz, "Electrostatic RF MEMS Tunable Capacitors with Analog Tunability and Low Temperature Sensitivity," *IEEE Transactions on Microwave Theory and Techniques*, pp. 1254–1257, May 2010.

[35] C. D. Patel and G. M. Rebeiz, "High-3 b/4 b RF MEMS Digitally Tunable Capacitors for 0.83 GHz Applications," *IEEE Microwave and Wireless Components Letters*, vol. 22, no.8, pp. 394–396, Aug. 2012.

[36] B. Lacroix, A. Pothier, A. Crunteanu, C. Cibert, F. Dumas-Bouchiat, C. Champeaux, A. Catherinot, and P. Blondy, "CMOS compatible fast switching RF MEMS varactors," *Proceedings of the 36th European Microwave Conference*, pp. 1072–1075, Sep. 2006.

[37] A. Grichener and G. M. Rebeiz, "High-Reliability RF-MEMS Switched Capacitors With Digital and Analog Tuning Characteristics," *IEEE Transactions on Microwave Theory and Techniques*, vol. 58, no.10, pp. 2692–2701, Oct. 2010.

[38] H. Zhangl, M. Li, D. Zhang, and N. C. Tien, "A Process Research for Integrated RF Tunable filter," *Proceedings of the 1st IEEE International Conference on Nano/Micro Engineered and Molecular Systems*, pp. 1449–1452, Jan. 2006.

[39] S. K. Lahiri, H. Saha, and A. Kundu, "RF MEMS SWITCH: An overview at a glance," *International Conference on Computers and Devices for Communication*, Dec. 2009.

[40] Peregrine Semiconductor, *San Diego, CA, USA, www.psemi.com.*

[41] Peregrine Semiconductor, *Datasheet PE42556 Flip Chip.*

[42] C. Demerjian, "Nvidia chips show underfill problems," *The Inquirer*, Dec. 2008.

[43] Omron Corporation, *Kyoto, Japan, www.omron.com.*

[44] Omron Electronic Components, "White Paper: RF MEMS Switch: What You Need to Know, Structure and Usage of OMRON MEMS Switch 2SMES-01,"

[45] Radant MEMS, *www.radantmems.com.*

[46] Radant MEMS, *Datasheet RMSW220HP, SPDT High Power, RF-MEMS Switch, DC to 40 GHz.*

[47] D. M. Pozar, *Microwave Engineering.* second ed., 1998.

[48] Center for Integrated RF Engineering (CIRFE), University of Waterloo, Waterloo, Ontario, Canada, N2L 3G1, http://www.cirfe.uwaterloo.ca

[49] P. Scheele, F. Goelden, A. Giere, S. Mueller, and R. Jakoby, "Continuously Tunable Impedance Matching Network Using Ferroelectric Varactors," *IEEE Transactions on Microwave Theory and Techniques*, May 2005.

[50] M. Schmidt, E. Lourandakis, A. Leidl, S. Seitz, and R. Weigel, "A Comparison of Tunable Ferroelectric Π- and T-Matching Networks," *Proceedings of the 37th European Microwave Conference*, Oct. 2007.

[51] H. Maune, M. Sazegar, and R. Jakoby, "Tunable Impedance Matching Networks for Agile RF Power Amplifiers," *IEEE Transactions on Microwave Theory and Techniques*, Nov. 2011.

[52] Tayo Yuden, www.t-yuden.com, *Datasheet HK10052N2S-T Multilayer Chip Inductors for High Frequencies Applications.*

[53] R. C. Jaeger, *Introduction to Microelectronic Fabrication, Chapter 2: "Lithography".* second ed., 2002.